REPORT

Development of a Recovery System for Metals and Acids from Pickling Baths using Nanofiltration and Crystallisation

Kåre Tjus Rune Bergström Uwe Fortkamp, IVL
Kerstin Forsberg Åke Rasmuson, KTH
B1692
October 2006

Rapporten godkänd
2007-03-14

Lars-Gunnar Lindfors
Forskningschef

IVL Swedish Environmental Research Institute

Report Summary

Organization

IVL Swedish Environmental Research Institute Ltd.

Address

P.O. Box 21060
SE-100 31 Stockholm

Telephone

+46 (0)8-598 563 00

Project title

Project sponsor

Author

Kåre Tjus Rune Bergström Uwe Fortkamp Kerstin Forsberg Åke Rasmuson

Title and subtitle of the report

Development of a Recovery System for Metals and Acids from Pickling Baths using Nanofiltration and Crystallisation

Summary

Within the project a possible combination of techniques for recovery of metals and acids from stainless steel pickling has been investigated, as there is a lack of cost and energy efficient methods that allow recycling of both metals and acids today. Crystallisation and nanofiltration were combined in order to separate the metals as metal fluorides and recycle nitric and hydrofluoric acid to the pickling bath.

A total treatment concept will also include the thermal treatment of the crystals, in order to gain metal oxides that can be reused. The fluorides will be recovered as HF from the exhaust gas. This thermal treatment has not been investigated in this project, but it should be possible to adapt existing techniques for that.

Experiments in laboratory scale were performed in order to increase understanding of the processes and for design of a pilot plant. A Pilot plant was built within the project. Process liquids from two stainless steel companies in Sweden were investigated with the pilot plant.

The experiments were used for recommendations on full-scale solutions as well as rough estimations on energy and cost savings. Tests for a longer period of time would be needed in order to be able to assess the life-time of the equipment and performance stability better, but the results show that the techniques could be used for metal separation to allow recycling of acids and prepare for metal recovery. The results also indicate possible energy savings when installing the system. Investigations from a parallel project show promising results regarding the on-line measurement of concentrations, which will allow a more efficient control of the process

Keyword

nanofiltration, crystallisation, FeF_3, iron fluoride, metal fluorides, pickling acid

nanofiltrering, kristallisation, metallfluorider, betsyra

Bibliographic data

IVL Report B1692

The report can be ordered via

Homepage: www.ivl.se, e-mail: publicationservice@ivl.se, fax+46 (0)8-598 563 90, or via IVL, P.O. Box 21060, SE-100 31 Stockholm Sweden

Contents

1 Background

Totally 900 000 tonnes of stainless steel are produced in Sweden yearly. When stainless steel is produced pickling baths of hydrogen fluoride, HF, and nitric acid, HNO_3, are used to clean the steel from oxide scales. They are originating from the preceding heat treatment in the steal forming processes. The pickling acid bath is used as long as possible, new acid is added continuously to replace the acids that are consumed by the metal cleaning process. Due to increasing high metal concentrations and high content of metal oxides, the pickling baths have to be replaced at least partly at certain intervals.

The main disadvantage of the high metal concentrations is an increased risk to get metal fluoride sludge in the bath. The concentration of metals in the dumped baths varies between 25 to over 50 grams per litre, this is due to a higher solubility of iron at lower acid concentrations and vice versa. This production gives rise to approximately 18 000 tonnes of metal hydroxide sludge each yearly. Today this sludge is mainly deposited. With this situation, it is of interest for stainless steel producers to reduce the amount of sludge generated, to recycle acids and find a way of separation of metals from the pickling bath.

Some techniques used today to recover acids and metals to prolong the life time of the pickling baths are:

- Filter presses for continuously removal of oxide scales. The filter press can remove particles from the pickling bath. Dissolved metals are not separated, except for the liquid fraction in the filter cake.

- Acid retardation in combination with precipitation is a common method for pickling bath treatment. The acid retardation allows a partly recovery of acids, the metals are precipitated creating a hydroxide sludge. Nitrates from the nitric acid are not separated in the precipitation step

- Electrodialysis has been added to the acid retardation treatment in order to allow a better recovery of nitrates. Still, metals are not recovered, but metal hydroxide sludge is produced.

- Electrodialysis with bipolar membranes has been used in after precipitation of pickling baths in order to recover the acids from their salts. This method allows the acid recycling, but is relatively expensive due to high membrane costs for the bipolar membranes. Metal hydroxide sludge is produced

- Evaporation and crystallisation in combination with thermal treatment for metal recovery. The process allows the recycling of both metals and acids. There has been one installation which has been shut down together with the factory closure. The evaporation step is more energy demanding than a nanofiltration step, and has different separation characteristics.

- Thermal treatment of the pickling bath is another option, for example by spray-roasting. The treatment allows recycling of hydrofluoric acid and metals, but an expensive exhaust gas cleaning is needed for the nitrous gases, not allowing recycling nitric acid.

- The Outokumpu process uses sulphuric acid is used to recover hydrofluoric acid. The process includes many process units like evaporation, crystallisation, and precipitation. The technology uses two precipitation steps in order to precipitate nickel separately.

- Sludge treatment is another technique handling metal hydroxide sludge. It is used to produce calcium fluoride from the sludge that could be used instead of fluorspar as a sludge forming agent in the steel making process.

All the above mentioned processes have certain disadvantages. In many cases it is not possible to recover both acids and metals and to avoid metal sludge. The proposed process that has been investigated in this project is a process integrated solution that avoids waste streams. It combines a concentration step with nanofiltration and a separation step with crystallisation. The concentration step is used in order to increase the supersaturation and improve the crystallisation conditions. Figure 1 shows the proposed nano hybrid combination. The process is quite similar to the treatment including evaporation.

Evaporation has been reported earlier as possible technology for the concentration step [Krepler, 1978]. Nanofiltration is attractive compared with evaporation due to its lower energy consumption. There is also a risk to get an uncontrolled crystallisation when evaporation is used as a pre-treatment before crystallisation. Besides, earlier work at IVL has pointed out that there is a risk to get a high content of acids within the crystals produced, probably due to a too rapid crystal growth. A disadvantage of many nano membranes is their possible short lifetime, which has been found for these membranes in the very aggressive pickling acid solutions.

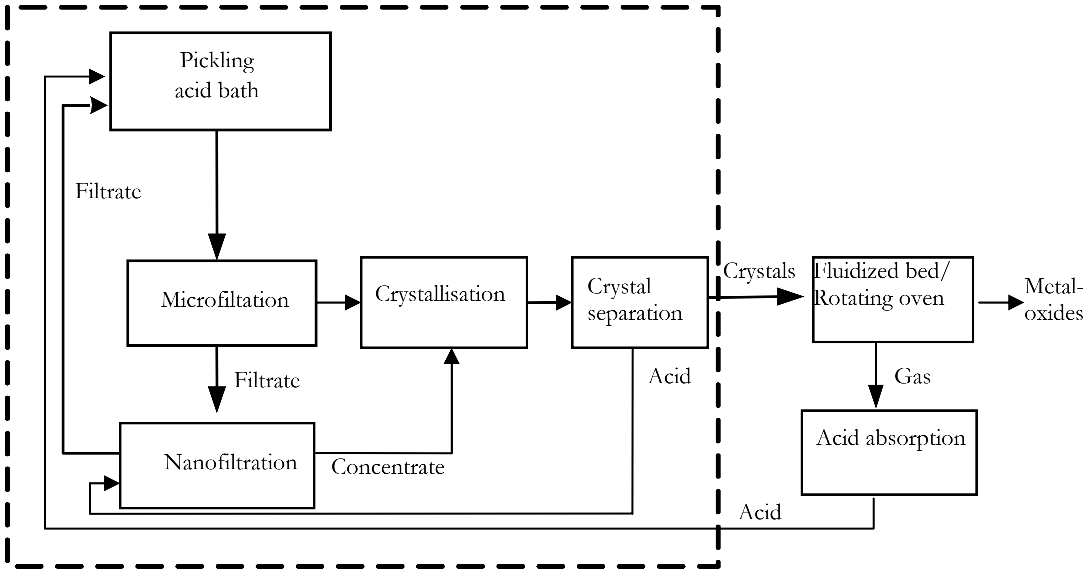

Figure 1 Schematic design of a hybrid system for recovery of acid and metal oxides from the pickling bath. Dotted square indicates the techniques that have been investigated in this study.

Crystallisation of metal fluorides has been studied by a number of authors. Iron fluoride trihydrate crystallisation has been studied since it offers a method for separating iron ions from spent pickling baths [Krepler, 1978], [Fortkamp et al., 2002, 2003]. The dimorphic aluminium fluoride trihydrate crystals are thought to be isostructural with the dimorphic iron (III) fluoride trihydrate crystals

[Chupas et al., 2003]. The chemical properties of aluminium ions and trivalent iron are similar owing to their similar radii and acid-base properties. Precipitation of aluminium fluoride trihydrate has been studied much due to the extensive use of anhydrous aluminium fluoride for adjusting the melt composition in the production of aluminium by the Bayer process. Large amounts of anhydrous fluoride are prepared by calcination of the trihydrate, which is formed by precipitation from an aqueous solution.

A more comprehensive review of the properties and crystallisation of metal fluoride hydrates can be found in the licentiate thesis "*Crystallisation of iron fluoride trihydrate from mixed acid solutions*" [Österdahl, 2003].

The whole process concept also includes a thermal treatment in order to allow the recycling of metals and fluorides that are bound as metal fluorides in the crystals. This study though, focuses on the nanofiltration and crystallisation steps as these are regarded to have the largest development needs. A full-scale installation would also benefit from on-line analysis of concentrations in order to control the whole process efficiently. There are parallel activities going on, which are shortly described in this report.

The project has been performed with support from the Swedish EPA, the Swedish Energy Authority, Outokumpu Stainless (called OKS in this report) and Sandvik Materials Technology (called SMT in this report). They have also contributed with valuable input to the discussions in the project.

2 Laboratory experiments

2.1 Crystallisation

The aim with the laboratory work was to investigate the crystallisation of metal fluoride hydrates from mixed hydrofluoric acid and nitric acid solutions (100 ml scale) in order to gain knowledge needed for the design of a pilot plant (10 L scale). The solubility and crystal growth of β-$FeF_3 \cdot 3H_2O$, which is the thermodynamically stable iron fluoride hydrate at prevailing conditions, have been investigated at different solution compositions and temperatures. Iron fluoride trihydrate crystallises slowly even at high supersaturation and high temperature. Therefore, it is of technological importance to study its growth kinetics. The crystal growth mechanism and kinetics have been studied by performing isothermal seeded desupersaturation experiments [Österdahl and Rasmuson (II), 2006]. Solubility measurements together with chemical speciation calculations have been performed in order to express the true supersaturation driving force [Österdahl and Rasmuson (I), 2006]. Primary nucleation experiments can be used to obtain the crystal-solution interfacial energy. Induction time is also of direct industrial interest [Österdahl et al., 2006].

2.1.1 Iron (III) fluoride trihydrate

Iron (III) fluoride trihydrate exist in two polymorphic forms, α- and β-$FeF_3 \cdot 3H_2O$. The β-phase is the thermodynamically stable form in the temperature interval studied here, 30-50°C, and also at room temperature (Dézsi et al., 1987). The α-phase is kinetically favoured and will usually precipitate first in a supersaturated solution at temperatures below about 30°C. Wang (1992) studied precipitates from different HF and HNO_3 pickle liquors and identified the iron fluoride phases found as $FeF_2{\cdot}4H_2O$ and $FeF_3{\cdot}3H_2O$ by X-ray diffraction. Karraker and Smith (1992) writes that the structure reported by Penford and Taylor (1960) as $FeF_2{\cdot}4H_2O$ is actually the α-phase of $FeF_3{\cdot}3H_2O$. Thus it is very probable that Wang found the α- and β-phase of $FeF_3{\cdot}3H_2O$.

When heated β-$FeF_3{\cdot}3H_2O$ starts to decompose at 140°C, forms $FeF_3{\cdot}H_2O$ at about 200°C and turns into Fe_2O_3 at about 500°C (1atm) (Macheteau and Charpin 1972, Dézsi et al. 1987).

2.1.2 Solubility measurements

The solubility of β-$FeF_3{\cdot}3H_2O$ was determined in solutions of different hydrofluoric acid (1-6molal) and nitric acid (0-7 molal) concentrations at 30, 40 and 50°C.

2.1.3 Solubility of Nickel and Chromium

Nickel is known to precipitate as $NiF_2{\cdot}4H_2O$ from pickle bath solutions (Reddy et al. 1991). The solubility of $NiF_2{\cdot}4H_2O$ in water is insensitive to temperature changes, e.g. the solubility at 10°C is 2.49g/100g solution and at 90°C it is 2.52g/100g solution (Silcock, 1979). No solubility data of $NiF_2{\cdot}4H_2O$ in pickle bath acid could be found in literature. Several different chromium (III) fluoride hydrates are known to crystallize from aqueous solutions depending on the reaction conditions. Chromium (III) is known to co-precipitate with iron from pickle bath solutions in the crystal form of $CrF_3{\cdot}3H_2O$ (Reddy et al. 1991). No solubility data of $CrF_3{\cdot}3H_2O$ in pickle bath acid could be found in literature. It also exists a family of crystals with the general formula: $Me(II)Me(III)F_5{\cdot}7H_2O$. In order to precipitate these crystals negatively charged Me(III) fluoride complexes must exist in the solution.

2.2 Method

The solubility experiments were performed by adding different acid mixtures to 14 ml polypropylene (PP) test tubes filled with β-$FeF_3{\cdot}3H_2O$ crystals in excess. The test tubes were closed with stoppers and also sealed up with Parafilm to prevent evaporation losses. The test tubes were placed in a water bath (Julabo MD, ±0.01°C). Each solution was stirred with a magnetic stir bar. Solution samples taken at equilibrium conditions were analysed for total iron using inductively coupled plasma atomic emission spectroscopy (ICP-AES JY 24, Jobin Yvon). The measurements were made at 239.204 nm.

Several introductory experiments were performed in order to learn how to best synthesize β-$FeF_3{\cdot}3H_2O$ crystals. The crystals of β-$FeF_3{\cdot}3H_2O$ finally used in the experiments was prepared by dissolving freshly precipitated ferric hydroxide in 20w% hydrofluoric acid followed by evaporation crystallisation [Teufer, 1964]. The pink precipitate was vacuum filtered and washed with water at 50°C and dried by leaving the crystal mass for several days in an incubator at 60°C. The crystals were identified as β-$FeF_3{\cdot}3H_2O$ by X-ray diffraction (XRD, Bruker-Nonius KappaCCD Single Crystal Diffractometer).

2.2.1.1 Results

Figure 2 shows how the solubility in terms of total iron concentration increases as the temperature increases in solutions of 0.9 mol/kg HF (free acid) and 0.9 mol/kg HNO_3.

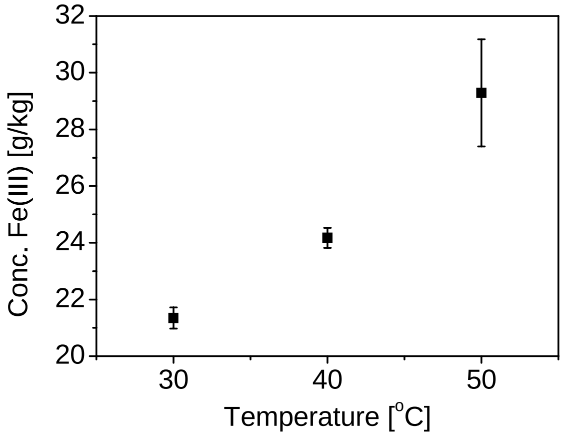

Figure 2 Solubility of β-$FeF_3 \cdot 3H_2O$ in terms of total iron concentration in 0.9 mol/kg HNO_3 and 0.9 mol/kg HF. Each data point is a mean of two measurements and the 95% confidence interval is shown for the measurements at each temperature.

The total iron concentration at equilibrium ranges from about 1 to 35 g/kg solution, taken in to account all the performed experiments. In the range of investigated conditions, the solubility in terms of total iron content decreases with increasing concentration of hydrofluoric acid and nitric acid. Figure 3 shows how the solubility at 30°C varies with acid concentration, the data values are given in Appendix 1.

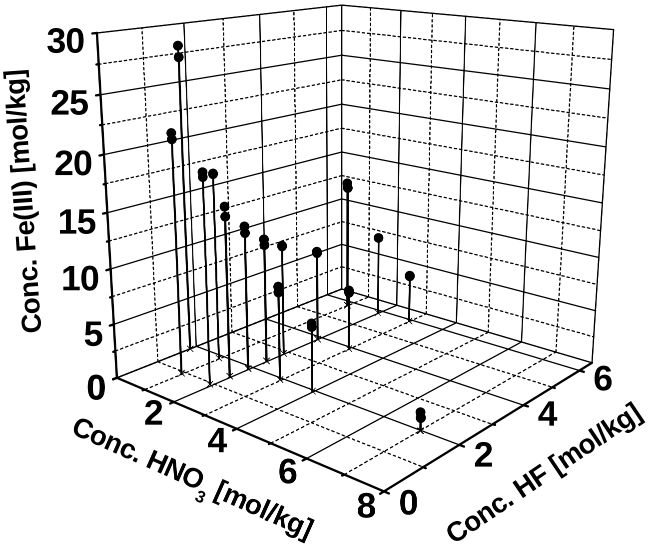

Figure 3. Solubility of β-$FeF_3 \cdot 3H_2O$ in terms of total iron concentration at 30°C in different mixtures of HNO_3 and HF

The results can be explained by examining the chemical speciation in the solutions [Österdahl and Rasmuson, 2006]. The concentration of the complex $FeF_3(H_2O)_3$ is constant as the hydrofluoric acid concentration varies in solutions in equilibrium with β-$FeF_3 \cdot 3H_2O$ crystals at a specific temperature and ionic strength. The ionic strength is mainly determined by the nitric acid concentration. Figure 4 shows how the concentration of the different iron complexes changes as the free fluoride ion concentration varies in solutions of 1 mol/kg HNO_3 at 30°C. As can be seen the total iron concentration decreases due to a decreased amount of positively charged complexes as the hydrofluoric acid concentration increases.

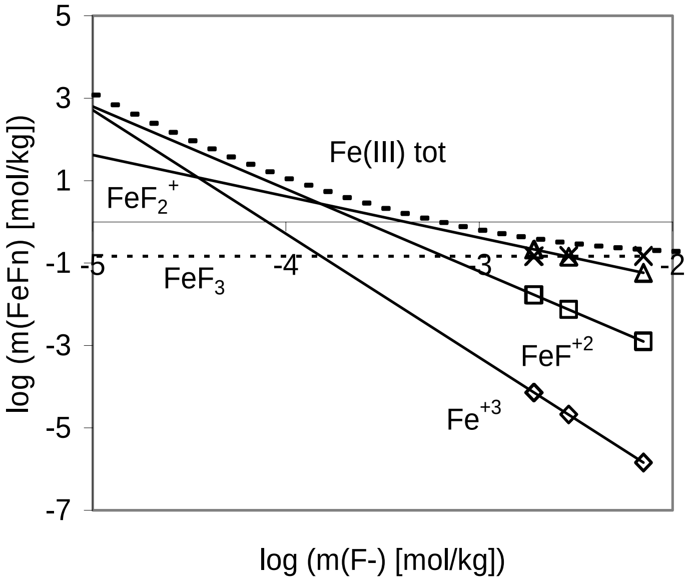

Figure 4. Iron fluoride species distribution (n= 0- 3) with varying free fluoride ion concentration at equilibrium with β-$FeF_3 \cdot 3H_2O$ crystals in a 1 mol/kg HNO_3 solution at 30°C.

2.2.2 Induction time measurements

2.2.2.1 Method

The Primary nucleation of β-$FeF_3 \cdot 3H_2O$ was studied in solutions of 2- 3 mol/kg HF and 3 mol/kg HNO_3 at 50°C and 55°C. Supersaturated solutions were prepared by mixing appropriate amounts of iron nitrate ($Fe(NO_3)_3 \cdot 9H_2O$, PA, >99%), de-ionised filtered water, 65,4w% HNO_3 and 40,1w% HF. The supersaturation ($S= c_{Fe(III)}/c_{Fe(III)}{}^*$) in the prepared solutions were in the range expected in an industrial iron fluoride trihydrate crystallisation process, i.e. $1.1< S< 2.0$. The supersaturated solutions were added to 14 ml polypropylene (PP) test tubes. The test tubes were closed with stoppers, sealed up with Parafilm to prevent evaporation losses and placed in a water bath (Julabo MD, ±0.01°C). Each test tube was stirred with a magnetic stir bar at 400 rpm. The induction time was determined by observing when the first particles became visible to the naked eye.

2.2.2.2 Results

The nucleation event was difficult to observe. The induction times were long and the crystals grew very slowly. The results are presented in Table 1. The induction time in the experiment at 55°C in 2 molal HF, 3 molal HNO_3 and 55.8g Fe/kg (S= 4.0) was 30 minutes.

Table 1. Results of induction time experiments at 50°C in solutions of 3 molal HF and 3 molal HNO_3

Sample	Iron conc. [g/kg]	Supersaturation	Induction time [h]
A	11.4	1.1	150
B	13.5	1.3	65
C	15.6	1.5	40
D	17.7	1.7	20
E	19.7	1.9	10

The interfacial energy can be estimated from induction time measurements [Österdahl, 2003]. Making such an evaluation using the experimental data gives an interfacial energy of 3.6mJ/m^2, which is very low. According to a correlation of interfacial energy with solubility [Nielsen, 1984] the interfacial energy of β-$FeF_3 \cdot 3H_2O$ can be approximated to 31mJ/m^2. In order to determine the interfacial energy from experimental data the observed induction time must be governed by the actual induction time of nucleation. The observed induction time in primary nucleation experiments consist of the relaxation time, the nucleation time and the time for the crystals to grow to a visible size. As the growth rate measurements showed, the β-$FeF_3 \cdot 3H_2O$ grow slowly. Suspensions of particles that have diameters greater than 1micron are visible to the naked eye. The growth times at each supersaturation for which induction times have been measured employing the crystal growth results can be calculated. At a supersaturation of 1.5 and a temperature of 50ºC the growth rate is 4×10^{-12} m/s (3 mol/kg HF and 3 mol/kg HNO_3). Thus, it takes about 36 hours for the crystals to grow 0.5micron. At S= 2 it takes 9 hours for the crystals to grow 0.5micron. These results suggest that the measured induction times mainly consist of the time for the crystals to grow to a visible size, thus the growth time can not be neglected. Since the growth rate is so slow it is reasonable to assume that the nucleation event takes place much earlier than reported in Table 1.

2.2.3 Crystal growth experiments

The purpose of the crystallisation experiments was to determine the influence of different parameters on the growth rate of iron fluoride trihydrate crystal growth. Important parameters to consider are pH, temperature, ionic strength, stirring effects and concentration of fluoride and metal ions.

2.2.3.1 Experimental Method

The crystallisation kinetics of β-$FeF_3 \cdot 3H_2O$ crystals was studied by performing seeded isothermal desupersaturation experiments. Supersaturated solutions were prepared by mixing 55g Fe/kg iron nitrate solution ($Fe(NO_3)_3 \cdot 9H_2O$, PA, >99%), de-ionised filtered water, 65.4 w% HNO_3 and 40.1 w% HF in plastic bottles (HDPE). The bottles were sealed and placed in a water bath held at a constant temperature. Each bottle was agitated with a magnetic stir bar (200 rpm). Directly after the preparation of the supersaturated solution a sample was taken to be analysed by inductively coupled plasma atomic emission spectroscopy (ICP-AES). Thereafter a specific amount of β-$FeF_3 \cdot 3H_2O$ crystals were added to each solution. After the addition of seeds the crystal growth was followed by taking samples of approximately 2 ml slurry from the solutions once every 60 minutes by a pre-heated syringe. The solutions were then quickly filtered through a PVDF-filter to bottles of de-ionised water and were diluted in two steps. The metal content was analysed by ICP. Total fluoride and nitrate concentrations were also measured in a few samples using ion chromatography employing an electrical conductivity detector.

The seed crystals used in the experiments were prepared as in the solubility experiments. They were very small (Figure 5).

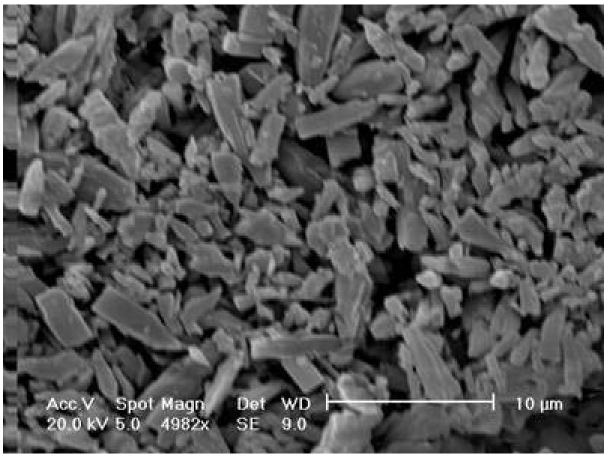

Figure 5. SEM picture of β-$FeF_3 \cdot 3H_2O$ seed crystals used in the growth experiments

2.2.3.2 Evaluation method

A connection of the macroscopic crystal growth rate with changes in supersaturation and temperature is the goal when examining the crystal growth. The macroscopic crystal growth rate is expressed as the rate of increase of the radius of the crystal, $G/\text{m} \cdot \text{s}^{-1}$. Depending on the crystal surface structure, supersaturation and temperature, different growth mechanisms might dominate. The results of the growth experiments in terms of iron consumption and supersaturation were fitted to two different equations, the theoretically based Burton-Cabrera-Frank (BCF) expression (equation 1.1) and an empirical power law equation (equation 1.2).

The BCF growth rate equation describes the growth as proceeding by surface diffusion of growth units across the face towards steps on the surface. The steps form spirals at the crystal surface. At low and moderate supersaturation the BCF equation can be written as:

$$G = \frac{dr}{dt} = k_2 (S-1)^2 \tanh\left(\frac{k_1}{k_2 (S-1)} \right) \quad (1.1)$$

where G is the linear rate of growth perpendicular to the face and S is the driving force available for surface integration. Often an empirical power law expression is used to relate the overall linear growth rate to the supersaturation. This expression is known to correlate experimental results well over narrow supersaturation ranges.

$$\frac{dr}{dt} = k_g (S-1)^g \qquad (1.2)$$

where k_g is an overall crystal growth rate constant. Unlike the parameters in the BCF-expression the growth order g in this equation has no direct fundamental significance. The power law equation is merely expressing the growth rate as a function of an overall concentration driving force, which is quite easily measured.

In the evaluation of the growth experiments it is assumed that all the crystals are of equal size and that the crystal shape and the number of crystals per kilogram solution are constant during growth. At these conditions the concentration decay can be related to the linear crystal growth rate according to [Qiu and Rasmuson, 1990]:

$$\frac{dc}{dt} = -\frac{dr}{dt}\frac{3W_0}{r_0 m}\left[1+\left((c_0-c)\frac{m}{W_0}\right)\right]^{2/3} \quad (1.3)$$

Where $dr/dt = G$ and is a function of the supersaturation and hence of the concentration. W_0 is the initial mass of crystals, r_0 the average radius of crystals assuming spherical shape, m the mass of the solution (kg). The crystal growth rate parameters were evaluated by direct non-linear parameter estimation [Österdahl and Rasmuson (II), 2006; Qiu and Rasmuson, 1990] in MATLAB (version 7.01). The crystal growth function (equation 1.1 or 1.2) and equation 1.3 is integrated numerically and the growth parameters are obtained by nonlinear curve-fitting (data-fitting) in the least-squares sense. The objective function to be minimized was defined as:

$$F = \sum_{j=1}^{m}\left(c(t_j)-c_j\right)^2 \quad (1.4)$$

Where c is expressed in terms of the free FeF_3 concentration (mol/kg) calculated by the chemical speciation computer program SSPEC [Fernando, 1990]. The ionic strength is taken to be constant during the growth period in the speciation calculations. The characteristic length of the crystal seeds is defined as the radius of a sphere with the same volume as the particle. The radius is calculated as: $r_0 = 3/(A_{sp}\times\varrho_c) = 9\times10^{-7}$m, using $\varrho_c=2321$ kg/m^3 [Teufer, 1964], A_{sp} is the specific surface area of crystals (m^2/g), measured as specific BET surface area of the crystal seeds: 1.44 m^2/g. This BET surface area is the mean of two measurements with 1.7 g seeds: 1.45 ±0.01 m^2/g and 1.6g seeds: 1.42 ±0.01 m^2/g. A measurement of the BET surface area of crystals after growth at 50°C (2.6g seeds: 1.47 m^2/g) showed that the surface area did not change appreciably during growth.

2.2.4 Results

Desupersaturation curves of two identical experiments are shown in Figure 6, as can be seen the experiments can be accurately reproduced. The figure shows how the concentration of FeF_3(aq) in the solution decreases with time while β- $FeF_3\cdot3H_2O$ is precipitated. In the experiments showed in Figure 6 the solutions in equilibrium with β- $FeF_3\cdot3H_2O$ crystals contain 0.12 mol FeF_3(aq)/kg solution.

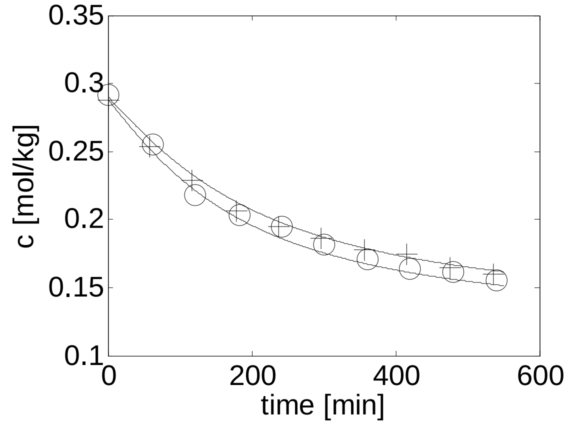

Figure 6. Concentration of FeF3(aq) as a function of time at 50°C in 6 mol/kg HF and 1.5 mol/kg HNO_3.

From the slope of the desupersaturation curves (e.g. the ones shown in Figure 6) crystal growth mechanisms and kinetics could be evaluated (as described above) at different conditions. Figure 7 shows how the growth rate depend on the supersaturation in a solution of 3 mol/kg HF and 3 mol/kg HNO_3 at 50°C expressed by equation 1.2 and the evaluated parameters at this conditions (g= 2.0, k_g= 1. 6×10^{-11} m/s) [Österdahl and Rasmuson (II), 2006].

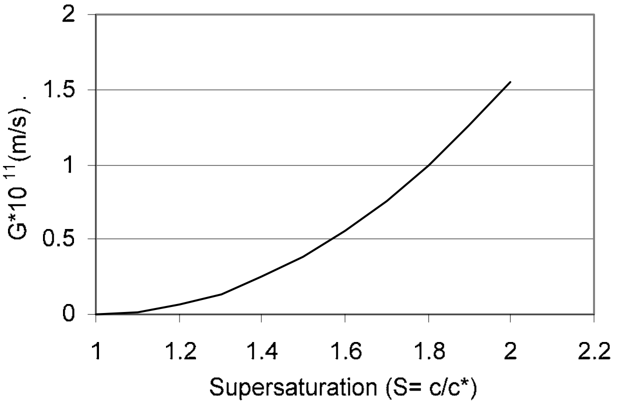

Figure 7. Linear growth rate as a function of supersaturation in a mixture of 3 mol/kg HF and 3 mol/kg HNO_3 at 50°C

By performing experiments at different stirring rates keeping all other variables constant the effect of stirring rate on the crystal growth rate could be investigated. These experiments showed that the stirring rate does not influence the crystal growth rate [Österdahl and Rasmuson (II), 2006].

The influence of temperature on the crystal growth rate was investigated by performing experiments at 30, 40 and 50°C. By evaluation of the results as described above the crystal growth rate could be calculated as a function of supersaturation and temperature using equation 1.2 and the Arrhenius relationship [Österdahl and Rasmuson (II), 2006]. The crystal growth rate as a function of temperature at a supersaturation of 1.5 is shown in Figure 8.

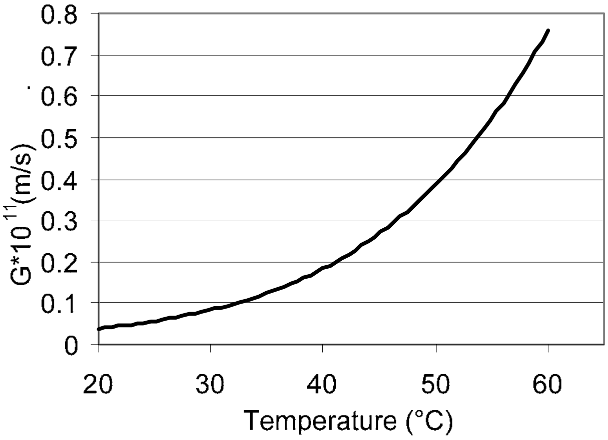

Figure 8. Linear growth rate as a function of temperature in a mixture of 3 mol/kg HF and 3 mol/kg HNO_3 at S= c/c_s= 1.5

Experiments at different nitric acid concentration and hydrofluoric acid concentration reveal that the acid concentration seems to influence the iron fluoride trihydrate growth rate. For example is the linear growth rate in a solution of 6 mol/kg HF and 3 mol/kg HNO_3 6.8 ×10-12 m/s while the growth rate in a solution of 3 mol/kg HF and 3 mol/kg HNO_3 is 3.9 ×10-12 m/s at the same supersaturation (S= 1.5) and temperature (50°C).

A number of additional experiments were performed where the influence of Ni(II) and Cr(III) on the growth rate of β-$FeF_3 \cdot 3H_2O$ were studied. The experiments show that Cr(III) co-precipitates with Fe(III). The crystal structure of the chromium precipitates in these experiments was identified as $CrF_3 \cdot 3H_2O$. Ni(II) will be present at high concentration in any crystallisation process since the solubility of $NiF2 \cdot 4H_2O$ in HF/HNO_3 solutions is high (>25g Ni(II)/L). The solubility of $NiF_2 \cdot 4H_2O$ is not expected to change appreciably with temperature in the range of 20°C to 50°C.

2.2.5 Conclusions

The solubility increases as the temperature increases. The solubility in terms of total iron concentration is also found to increase as the hydrofluoric acid and nitric acid concentration increases. The induction times for crystallisation were found to be long. However, there is uncertainty about the actual metastable range. The growth rate of iron fluoride trihydrate is low. The growth rate increases significantly with temperature, thus it is desirable to operate the pilot plant crystalliser at temperatures above room temperature.

2.3 Membrane filtration

Different nanofiltration membranes for separation of metals from acids have been investigated in laboratory experiments and in pilot plant tests. These tests were carried out in order to gain information about which membranes to study further and to get information about predicted lifetimes for the membranes.

Nanofiltration offers an, compared to other technologies, energy efficient way to separate dissolved components due to differences in size and charge. However, its use can be limited by instability of membranes to highly oxidising mediums such as pickling bath acid. The purpose of the nanofiltration experiments was to find membranes with good selectivity for metal ions as well as sufficient resistance against the strongly oxidising acid medium; i.e. membranes that could maintain a good flux (i.e. permeate flow rate) and a high retention of metal ions even after being in contact with mixed acid pickle liquor for longer periods of time.

2.3.1 Apparatus and Method

A half litre scale apparatus was constructed to perform nanofiltration-screening tests. The apparatus was made of Teflon inside to withstand the aggressive pickling acid, and stainless steel on the outside to withstand high pressure. The experimental set-up is shown in Figure 9. The applied pressure was monitored using a nitrogen gas pressure gauge.

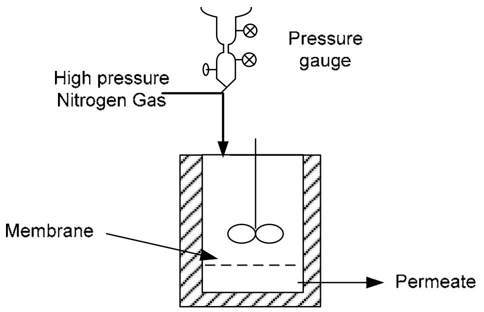

Figure 9. Experimental apparatus in half litre scale used to test the selectivity and acid resistance of different nanofiltration membranes

Initially the membrane performance was tested with aqueous solutions containing 1 g/l of $MgSO_4 \cdot 7H_20$ (Merck, pro analysis grade) in a similar unit made entirely of metal. The membranes were stored in pickling bath acid at 20ºC or 40ºC for various amounts of time (2 - 5 months) prior to the experiments. These tests were safer to perform since they did not involve filtration of hazardous HF and HNO_3 mixtures in the filtration step.

Batch membrane filtration experiments with pickling acid solutions were performed at temperatures between 20ºC and 44ºC. At the beginning of the experiments the half litre tank was filled with the desired pickling acid, and then a constant pressure was applied. The solution was continuously stirred at 500 rpm. Permeate samples were taken at regular intervals and the permeate flow was registered. During the tests the volume of acid in the container (the retentate) was decreased to about one third of the initial volume. At the end of the experiments the tank was emptied and carefully washed. The metal retention (r_m) for each experiment was calculated from the concentration in feed and permeate and is expressed as:

$$r_m = 1 - c_{permeate}/c_{feed}.$$

At low pH, the membrane is positively charged and thus no nitrate or negatively charged fluoride species retention is expected because of the electrostatic attraction.

Scanacon SA70 Acid Manager was used for analysis of concentrations of metals and acids. This equipment analyses dissolved metal concentration and free hydrofluoric and nitric acid concentrations by measuring H_3O^+ and F^- concentration with ion-selective electrodes and the solution density. The iron concentration was also measured using atomic absorption or ICP spectroscopy analysis. Conductivity of $MgSO_4$ solutions was measured with Multiline F/SET-3 from WTW (Wissenschaftliche Technische Werkstätten).

2.3.1.1 Membranes

The membranes used were supplied by three different companies, Koch Membrane Systems, GE Osmonics and Microdyn-Nadir. From Koch Membrane Systems different MP- Flat sheet (MPF) membranes of type code 34 were tested (delivered in 1999 and in 2003). From GE Osmonics the membranes KH, DK and DL (all delivered 2003) were tested. From Microdyn-Nadir N30F membranes were tested (delivered in 2004 and in2005).

Table 2. Membrane data from the manufactures are presented below

		pH	Temp. ºC	Max. Pressure	Rejection Glucose	NaCl
Koch Membrane systems	MP-34	0-14	max. 70	35 Bar	95%	35%
Microdyn - Nadir	OY NP030	0-12	max. 80			
					MgSO4	
Osmonics	Desal DK	1-11.5	max. 50	35 Bar	98%	
Osmonics	Desal DL	1-11.5	max. 50	35 Bar	96%	
Osmonics	Desal KH					

The membranes tested were either fresh after washing with water or stored several month in pickling acid at 20ºC or 40ºC with acid concentrations 1.3 M HF and HNO_3 1.8 M with a metal concentrations of approximately 20 g/l.

The membranes from Nadir were pre-treated at high-pressure prior to use, according to instructions from Microdyn-Nadir. During the experiments the metal concentration, the pressure, and the temperature were varied.

2.3.2 Results and discussion

Table 3 gives an overview of the membrane experiments. The last 4 experiments with the numbering Pxx are pilot plant experiments. Their results will be reported in chapter 3.

Table 3. Overview over laboratory tests with different membranes (VRF= volume reduction factor, HF content: free of not other explained), at No 6,7,8,9,12,13,15,16: the membrane was stored in pickling acid)

	Membrane	Pre-treatment	Metall-content g/l	HF M	HNO_3 M	Pressure Bar	Temp. ºC	VRF	Analysis method
T1	Osmonics Desal	-	25	3.65 total	2.8	40	20	1-1.2	Atomic Abs.
T2	MPF34, lev-99	-	25	2.55 total	2.5	40	40	1	Atomic Abs.
T3	MPF34, lev-99	-	35	1.6 total	2.1	40	40	1	Atomic Abs.
1	MPF34, lev-99	-	33	1.04	1.4	20	20	1-1.3	Scanacon
2	MPF34,lev-99	-	30	3.0	1.6	20	20	1-1.3	Scanacon
3	KH, Osmonics	-	31	1.0	1.2	20	20	1-1.2	Scanacon
4	DL, Osmonics	-	39.5	1.4	1.7	20	20	1-1.3	Scanacon
5	DK, Osmonics	-	36	1.0	1.2	20	20	1-1.4	Scanacon
6	MPF34,lev-99	2 month at 40º C,b	42.5	1.0	1.64	40	20	1-1.4	Scanacon
7	KH, Osmonics	3 month at 40º C,b							Scanacon
8	DL, Osmonics	4 month at 40º C,b							Scanacon
9	DK, Osmonics	5 month at 40º C,b							Scanacon
10	KH, Osmonics	-	42	1.3	1.8	40	20	1-1.8	Scanacon
11	MPF34,del-99	-	42	1.3	1.8	40	20	1-2.8	Scanacon
12	MPF34, del-03	3 month at 40º C,b	21	1.6	2.2	40	20	1-2.0	ICP Iron
13	MPF34, del-03	3 month at 40º C,b	32.5	1.6	2.2	40	40-44	1-1.6	ICP Iron
14	Nadir N30F del- 04	-	21	1.6	2.2	40	20	1-1.25	ICP Iron
15	Nadir N30Fl del-04	2 month at 40º C,b	36	2.4	2.2	40	40		ICP Iron
16	MPF34 ,del-03	5 month at 40º C,b	36	2.4	2.2	40	40		ICP Iron
P1a	MPS34,del-05	Micro-filtration	23	2.8	2.7	35	40	1	Scanacon
P1b	MPS34,del-05	Micro-filtration	48	2.7	2.5	35	40	2	Scanacon
P2a	NadirOY, NP030, del-06	Micro-filtration	26	2.5	2.4	40	50	1	Scanacon
P2b	NadirOY, NP030, del-06	Micro-filtration	35	2.5	2.3	40	50	2	Scanacon

2.3.2.1 MP34 membranes from KOCH

Three different membranes delivered 1999, 2003 and 2005; all with the designation MPF34 or MPS34 were part of the experiments. "F" is flat sheet and "S" Spiral wound membranes.

A metal retention of between 60 and 70 per cent was measured for the membrane delivered 1999. For the spiral membrane delivered 2005 the retention was over 90 per cent. Comparing the flux of the spiral membrane, delivered 2005, with the membranes delivered 1999 a decrease in flux (P1a and P1b compared with 11) can be noticed. It is logical to reach a lower flux and increased retention if the membranes pores are narrower.

It could be proved that the flux for one membrane is dependant of the metal content in the pickling acid. In Figure 10 below is the dependence shown for the membrane delivered 1999.

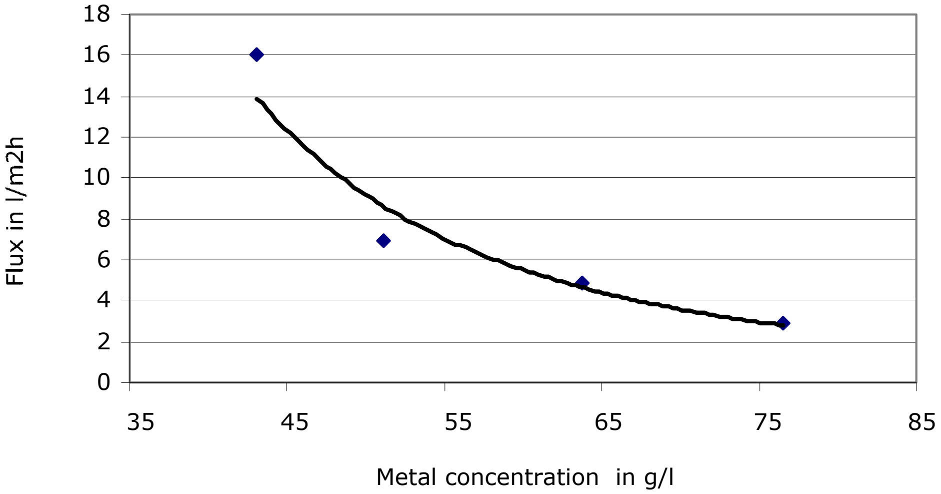

Figure 10 Permeate flux as function of metal concentration for a MPF34 membrane delivered 1999. The acid concentration is 1.3 M HF and 1.8 M HNO_3.

The flux decreases with increased metal concentrations. At 45 g/l the measured flux is 16 l/m^{2}h, at 75 g/l the flux has dropped to approximately 3 l/m^{2}h.

The flat sheet membranes were stored in pickling acid at 40 °C for 2 - 4.5 months. These tests were performed to investigate how well the membranes can withstand the acids. The tests showed a decrease in metal retention, which seems to increase by storage time.

For the flat sheet delivered 1999 an increase in flux after 2 months storage was noticed. Pores damaged by the acids probably cause this. The flow increased from 16 m^2/h to 40 m^2/h between 0 h and 2 month storage. For the flat sheet delivered 2003 the increase in flow was first noticed after 4.5 months storage. The flow increased from 6 m^2/h to 18 m^2/h between 2 month and 4.5 month storage. It seems that the membrane delivered 2003 can withstand acids better than the membrane delivered 1999.

Tests of flow rate and retention for these membranes were also conducted by using a solution of $MgSO_4$*7 H_2O for testing of the membrane performance. Also here the membranes were stored in a mixed acid (1.3 M HF and HNO_3 1.8 M, metal concentrations approximately 20g/l). In Figure 11 the results are presented.

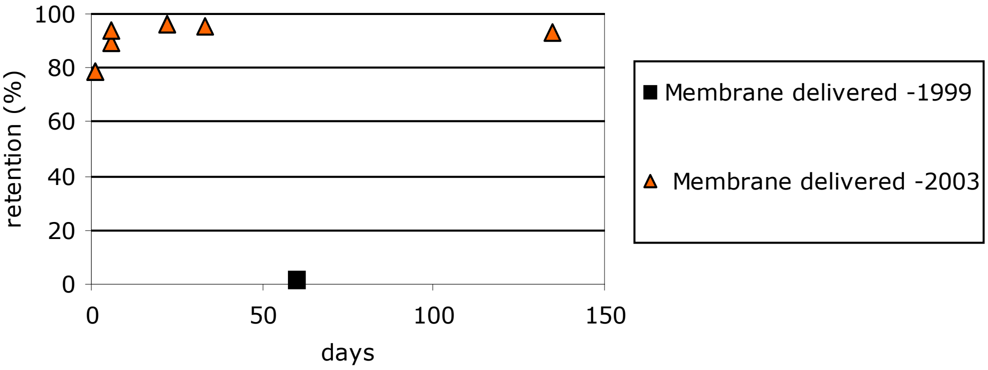

Figure 11 Retention of a 1g/l MgSO4 *7H20 solution for membranes (MP 34) stored in pickling acid at 40 °C is plotted against storage time (days). The retention was measured at room temperature and at 20 bars pressure.

For the membrane delivered 1999 it is obvious that the retention of $MgSO_4$ is almost zero after two months storage in pickling acid. In contrast hereto the membrane delivered 2003 is still giving a good retention after 135 days storing (4.5 month).

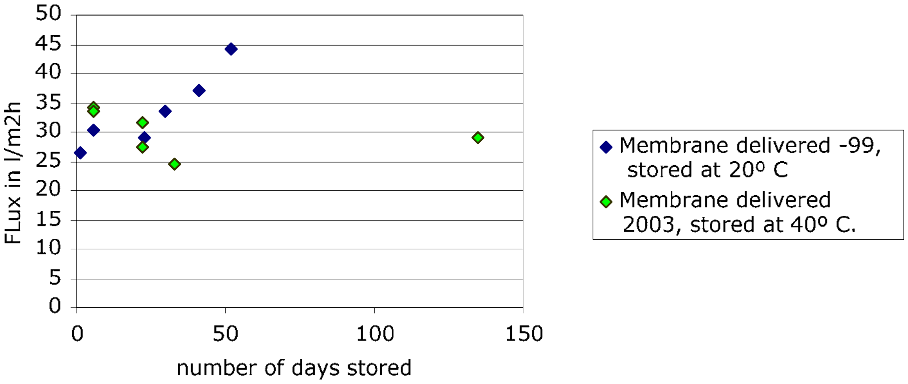

Figure 12. Flux as function of storage time for 1g/l $MgSO_4$ *$7H_20$ solution for membranes stored in pickling acid at 20° C and 40 °C. The flux was measured at room temperature and at 20 bars pressure.

The initial flux for both membranes was about the same for the two membranes. At storage at 20°C the flow increases by storage time for the membrane delivered 1999. For the membrane delivered 2003 no increase in flux could, initially, be observed by storage at 40 °C. A slight decrease could in fact be shown for this membrane for the first 40 days from 35 to 25 l/m^2h, deposited fluorides could cause this effect. After 4.5 month the flux has increased from 25 l/m^2h to 30 l/m^2h.

From these results it seems that the membrane delivered in 2003 have a better ability to withstand acids. It is obvious that the test with $MgSO_4$ solutions gives an indication of the behaviour of the membrane for the pickling system, but it does not fully predict the performance in pickling systems.

In table 3 results from the experiments are shown. The results from one spiral membrane experiment (P1a) in pilot scale are included for comparison.

Table 4. MP34 membranes, delivered different years from Koch (VRF= volume reduction factor, HF content: free of not other explained), at No 6,12,13,16: the membrane was stored in pickling acid)

	Membrane	Pre-treatment	Metal g/l	HF M	HNO_3 M	Pressure Bar	Temp ºC	VRF	Flow l/(m^{2}h)	Metals %	Analysis method
1	MPF34, lev-99	-	33	1.04	1.4 M	20	20	1-1.3	1.5	70	Scanacon
2	MPF34, lev-99	-	30	3.0	1.6 M	20	20	1-1.3	1.7	61	Scanacon
6	MPF34, lev-99	2 month at 40ºC,b	42.5	1.0	1.64 M	40	20	1-1.4	41	21	Scanacon
11	MPF34, del-99	-	42	1.3	1.8 M	40	20	1-2.8	16	60	Scanacon
12	MPF34, del-03	3 month at 40ºC,b	21	1.6	2.2 M	40	20	1-2.0	4.5	56	ICP Iron
13	MPF34, del-03	3 month at 40ºC,b	32.5	1.6	2.2 M	40	40-44	1-1.6	5.7	23	ICP Iron
16	MPF34, del-03	5 month at 40ºC,b	36	2.4	2.2 M	40	40		18	16	ICP Iron
P1a	MPS34, del-05	Microfiltration	23	2.8	2.7 M	35	40	1	7	99	Scanacon

2.3.2.2 Membranes from Osmonics:

Three different membranes from Osmonics were tested; KH, DL and DK. KH had a better retention for metals, 91 %, compared with flat sheet MP34. DK has a retention of about 74 % which is slightly higher than MP34 flat sheet membranes. DL had a lower retention, 32 %. Comparatively the flux is highest for the DL membrane. It was however found that none of the membranes from Osmonics could withstand storage in acid at 40°C for a longer time. After 2 months storage all the membrane pores were completely destroyed as the metal retention shows.

Table 5. Membranes from Osmonics (VRF= volume reduction factor, HF content: free of not other explained), at No 6,7,8,9: the membrane was stored in pickling acid).

	Membrane	Pre-treatment	Metal-content g/l	HF M	HNO_3 M	Pressure Bar	Temp ºC	VRF	Flow l/(m^{2}h)	Metals %	Analysis method
3	KH. Osmonics	-	31	1.0	1.2	20	20	1-1.2	0.3	91	Scanacon
4	DL. Osmonics	-	39.5	1.4	1.7	20	20	1-1.3	4.4	32	Scanacon
5	DK. Osmonics	-	36	1.0	1.2	20	20	1-1.4	0.44	74	Scanacon
6	MPF34.lev-99	2 month at 40ºC,.b	42.5	1.0	1.64	40	20	1-1.4	41	21	Scanacon
7	KH. Osmonics	3 month at 40ºC,b							high	0%	Scanacon
8	DL. Osmonics	4 month at 40ºC,b							high	0%	Scanacon
9	DK. Osmonics	5 month at 40ºC,b							high	0%	Scanacon
10	KH. Osmonics	-	42	1.3	1.8	40	20	1-1.8	4.4	82	Scanacon

2.3.2.3 Membrane from Nadir

One membrane from Microdyn-Nadir was investigated, N30 F. This membrane seems to withstand acids in a similar way as the MP34 membranes delivered 2003. However the metal retention was lower, approximately 30-40 %, for the Nadir membranes. The flux is as low as for the MP34 membrane delivered 2003, 4- 5 l/m²h at a metal concentration of 20 g/l.

In experiments with a spiral membrane from Nadir the retention was in the same order as for the flat-sheet membrane, but the flux was significantly higher than in the lab-scale experiments described here. A further discussion of these results is part of the pilot plant section.

Table 6. Membrane N30 F and NPO30 from Nadir (VRF= volume reduction factor, HF content: free of not other explained), at No 15, the membrane was stored in pickling acid.

	Membrane	Pre-treatment	Metall-content g/l	HF M	HNO_3 M	Pressure Bar	Temp. ºC	VRF	Flow l/(m²h)	Metals %	Analysis method
14	Nadir N30F del- 04	-	21	1.6	2.2	40	20	1-1.25	4.5	34	ICP Iron
15	Nadir N30Fl del-05	2 month at 40ºC,b	36	2.4	2.2	40	40		4.6	11	ICP Iron
P2a	NadirOY, NP030, del-06	Micro-filtration	26	2.5	2.4	40	50	1	49	40	Scanacon
P2b	NadirOY, NP030, del-06	Micro-filtration	35	2.5	2.3	40	50	2	43	40	Scanacon

2.3.2.4 Comparison of membranes

The membranes from different suppliers showed significant differences especially in the durability towards pickling acid. A possible explanation is that the producers used different materials to produce the membranes. Also, by different production processes, the surface properties and cut-off can be changed.

From the tests mainly two membranes were showing promising results for further investigations, as they might stand the acids for a longer time and be able to separate metal fluorides sufficiently:

- Koch MP- 34 and
- Nadir N30 F

3 Pilot plant experiments

3.1 Design of the pilot plant

The results from the laboratory scale experiments have been used to design a combined nanofiltration and crystallisation pilot plant. The set-up is shown in Figure 13.

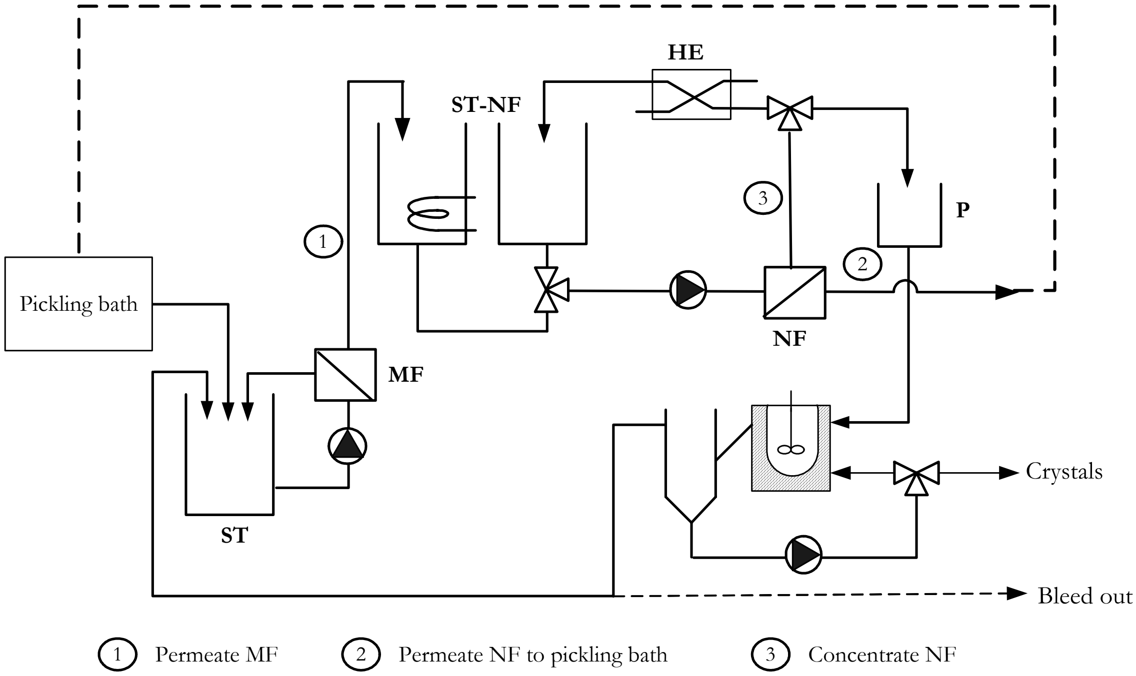

Figure 13 Flow chart of the pilot plant. MF= Microfiltation unit, NF= Nanofiltration unit, Cry= Crystallisation, ST-NF= Storage tanks for nanofiltration, P=Storage tank for concentrate, HE=Heat exchanger, ST Storage tank for crystal outlet/inlet from pickling bath.

The pilot unit for nanofiltration and crystallisation can be used to treat a small pickling bath or wasted acid. The permeate outlet can go back to the pickling bath. The pilot plant consists of 3 unit separation steps that are described in Table 7.

Table 7. Purpose of the unit operations used in the pilot plant.

Unit operation	Task/effect
Microfiltration (MF)	Separates particles, avoid problems in NF, no large effect on acid concentrations
Nanofiltration (NF)	Increase metal concentration in retentate, achieves a higher supersaturation for crystallisation, no large effect on acid concentrations
Crystallisation + sedimentation	Separates metals in solid form as crystals from the acids, some liquid remains in the crystal fraction

First the pickle liquor is filtrated by microfiltration to remove particles that otherwise would damage the nanofiltration membrane. The filtrate (1) is passed to a storage vessel where the solution is heated to a temperature in the range of 45 to 50 °C. The warm solution is then pumped to a feed and working tank from where it is transported to the membrane module using a high pressure pump. The membrane module consists of a 2.5 inches spiral wound nanofiltration membrane. The permeate stream (2) leaving the nanofiltration unit with a low metal content is removed from the system. It could be put back into a pickling bath. The retentate stream (3) with higher metal concentration is led back to the feed tank. The retentate stream can thus be circulated several times through the nanofiltration module until a desired metal concentration is reached. For continuous operation the retentate stream can also be split off to a separate storage vessel. The retentate solution is transported with a peristaltic pump at a desired rate (1 to 4 L/h) to a 10 L scale crystallisation vessel. The crystallisation vessel is equipped with four baffles. A single axial flow impeller placed in the centre of the vessel manages the agitation. The bottom of the crystalliser is slightly conical to avoid a stagnant zone beneath the impeller. The inlet pipe to the crystallizing vessel is placed near the stirrer where the turbulence is high, injecting the solution in the same direction as the bulk flow at this location (downwards). A sample withdrawal pipe is located halfway up the vessel. The temperature in the crystallisation vessel is measured using a polytetrafluoroethylene (PTFE) lined Pt 100 temperature sensor placed in the middle of the vessel near the wall. The solution leaving the crystalliser is circulated over a sedimentation vessel. From here crystal free solution continuously leaves the vessel at the top and the crystals at the bottom can be either continuously pumped back to the crystallisation vessel or removed from the system. Both the sedimentation and the crystallisation vessel are placed in a sealed, ventilated and thermostatic compartment. All vessels are constructed in polypropylene (PP); tubing is made of polyethylene (PE), Polyvinylchloride (PVC) or Marprene (trademark by Watson-Marlow). Parts of the high pressure pump and pressure regulators in the nanofiltration unit are made of Hastelloy C-22, this is the only material in contact with the mixed acid solution that is not plastic.

The nanofiltration and crystallisation part were equipped with a PLC system for automatic control (Simatic S7-300). The system was installed to allow control both at the equipment and remote from a PC.

The goal is to operate the pilot plant in a manner where metal is continuously separated at a moderate supersaturation ($1.5 \geq S \leq 2$). The nanofiltration is operated at (40- 50) °C and the crystallisation vessel is operated at 50 °C. There is an increased risk for primary nucleation in the tubes when raising the temperature. Raising the temperature in the crystallisation vessel will increase the crystallisation rate (see crystallisation section) but it will also involve more problematic waste gas and corrosion problems. The goal is to keep the supersaturation in both the nanofiltration equipment and the crystallisation vessel at moderate levels. As discussed in the crystallisation section the growth rate increases as the supersaturation is raised. However, at high supersaturation problems with scale formation is more probable.

3.2 Continuous crystallisation

3.2.1 Method

A combined nanofiltration and crystallisation pilot plant has been constructed where the metals are separated as metal fluoride crystals in a continuous crystallisation process. The equipment has been used to study and optimise the crystallisation process and the results from the pilot plant are to be used in the design of a large-scale plant. The retentate stream leaving the nanofiltration unit is circulated several times through the nanofiltration module until a desired metal concentration is reached. When the iron concentration is high enough the retentate stream is split off to a separate storage vessel. The retentate solution is then transported from the storage vessel at a desired rate (1 to 4 L/h) using a peristaltic pump to a 10 L scale stirred crystallisation vessel. The solution leaving the crystalliser is circulated over a sedimentation vessel. From here crystal free solution continuously leaves the vessel at the top and the crystals at the bottom can be either continuously pumped back to the crystallisation vessel or removed from the system.

Three experiments were performed in the pilot plant using pickle bath liquor delivered from either OKS (Avesta) or SMT (Sandviken).

3.2.2 Apparatus

The crystalliser has a diameter of 0.22 m and the sedimentation vessel has a cross section area of 2.6 dm^2. The crystallisation vessel is equipped with four baffles. The agitation is managed by a single axial flow impeller placed in the centre of the vessel pumping downwards. The bottom of the crystalliser is slightly conical upwards to avoid a stagnant zone beneath the impeller. The feed tube in the crystallizing vessel is placed near the stirrer where the turbulence is high, feeding the solution in the same direction as the bulk flow at this location (downwards). A sample withdrawal tube is located halfway up the vessel. The temperature in the crystallisation vessel is measured using a polytetrafluoroethylene (PTFE) lined Pt 100 temperature sensor placed in the middle of the vessel near the wall. Both the sedimentation and the crystallisation vessels are placed in a sealed, ventilated and thermostatic compartment. All vessels are constructed in polypropylene (PP). Tubing is made of polyethylene (PE), Polyvinylchloride (PVC) or Marprene (Trademark of Watson-Marlow).

3.2.3 Sampling and analyses

Sampling is performed by sucking up solution through the sample withdrawal tube using a syringe. Before each sampling occasion air is blown through the tube to empty it from solution. If the purpose of the sampling is to measure acid concentration or metal ion concentration the solution is immediately filtrated through a PVDF filter (0.2 μm, Acrodisc) and diluted in water. If the purpose is to obtain a sample of crystals the crystals are separated from the solution by vacuum filtration with filter paper VWR collection grade 454. The crystals are washed with water. The metal concentration in solution is measured by inductively coupled plasma atomic emission spectroscopy (ICP-AES, JY 24 Jobin Yvon). Hydrofluoric acid and nitric acid concentration is determined using a SA70 Acid Manager (Scanacon). Crystals are identified by X-ray diffraction.

3.2.4 Results

An overview of the performed experiments is given in Table 8.

Table 8. Conditions for the pilot plant experiments. The acid and total metal content reported below is the mean values of the ingoing concentrations during the whole runtime.

Exp.	HF M	HNO_3 M	Solubility Fe (c*) g/l	Total metal content g/l	Temperature °C	Flow rate l/h	Initial magma density w%	Run time h
1	2.6	2.4	13	44	40 - 45	3.0	1.4	24
2	2.6	2.7	13	37	45 - 50	1.5	7.4	36
3	1.9	2.4	15	41	45 - 50	1.3	15	48

In the first experiment the solution was seeded with precipitates and grinded scale from spent pickle liquor. Clear solution could easily be separated in the sedimentation vessel. The residence time during the experiment was 3.3 h. Experiment 1 was stopped already after 24 hours since the recirculation tube became clogged with crystals. Inspection after the experiment showed that crystals had grown on the lower inclined walls of the sedimentation tank. There had been no growth of crystals on the walls or on other parts in the stirred crystallisation vessel. However there were a lump of crystals at the bottom of the tank, indicating that the stirring had been insufficient. The experiment was evaluated and measures were taken.

The pickle bath liquor used in experiment 2 was delivered from the OKS steel plant in Avesta. Experiment 2 was conducted at lower supersaturation and a higher recirculation flow rate was used than in experiment 1. Crystals that had been crystallised from spent pickle bath liquor were used as seeds (green crystals of $FeF_3 \cdot 3H_2O$ with unknown chromium content). Clear solution could easily be separated in the sedimentation vessel (β-$FeF_3 \cdot 3H_2O$ has a density of 2.3 g/cm^3). The residence time during the experiment was 6.7 h. One crystal sample was taken at the start of the experiment. The crystals were filtrated by vacuum, washed with water and then dried in a furnace at 50°C. Samples of clear solution were taken of the incoming solution and by filtration of the solution in the crystalliser at the start of the experiment. After 31 hours a second sample of clear solution was taken from the crystalliser. The ingoing solution consisted of 24.5 g/L Fe(III) and 8.4 g/L Cr(III). The metal concentrations in the crystalliser during the experiment are presented in Table 9. The magma density, i.e. amount crystals per amount total liquid, was measured at the beginning and at the end of the experiment. The magma density increased from 7.4 vol% at the beginning of the experiment to 9.3 vol% the next day (after 30 h). The experiment was stopped already after 36 hours due to a stop in the recirculation flow.

Table 9. Fe(III) and Cr(III) content in the crystalliser during experiment 2.

Time h	c Fe (III) g/l	c Cr (III) g/l	Supersaturation Fe(III), c/c*
0	17.6	8.2	1.4
31	20.2	8.0	1.6

The pickle bath liquor in experiment 3 was delivered from SMT steel plant in Sandviken. The crystals from experiment 2 were used as seeds. The recirculation flow rate was the same as in experiment 2. Clear solution could easily be separated in the sedimentation vessel. The solution was filtrated to remove larger lumps of crystals that had formed during experiment 2. The residence time during the experiment was 7.7 h. The first sample of filtrated solution was taken from the incoming solution and from the crystalliser 16 hours after start. The incoming solution consisted of 37.8 g/L Fe(III) and 3.7 g/L Cr(III). The second sample of filtrated solution was taken 39 hours after start and the last sample was taken after 45 hours at the end of the experiment. The metal concentrations in the crystalliser during the experiment are presented in Table 10. A crystal sample was taken 39 hours after start. The crystals were filtrated by vacuum, washed with water and dried in an oven at 50°C. Powder diffraction identified the crystal structure as β-$FeF_3 \cdot 3H_2O$. The magma density was 15 vol% at the beginning of the experiment and 31 vol% after 45 hours at the end of the experiment. The experiment was stopped after running for 45 hours without problem.

Table 10. Fe(III) and Cr(III) content in the crystalliser during experiment 3.

Time h	c Fe (III) g/l	c Cr (III) g/l	Supersaturation Fe(III), c/c*
16	25.0	4.0	1.7
39	27.1	3.7	1.8
45	26.7	3.6	1.8

3.2.5 Discussion

The pilot plant experiments show that it is possible to separate iron from pickle bath solutions by crystallisation of $FeF_3 \cdot 3H_2O$. The magma density increased during all the experiments. In three experiments between 54 and 72 litres of solution passed through the crystalliser.

The first experiment was performed using seed material that partly consisted of oxide scale. The magma density was also lower in the first experiment then in experiment 2 and 3. The particles in experiment 1 were relatively large and were transported slowly with the solution through the recirculation tube. The low transport rate combined with high supersaturation led to that the recirculation tube became plugged. The problem was solved by increasing the recirculation rate and operating the crystalliser with higher magma density and using particles consisting of $FeF_3 \cdot 3H_2O$ crystals and no oxide scale.

Laboratory experiments have shown how the crystal growth rate of β-$FeF_3 \cdot 3H_2O$ increases with increasing supersaturation (Figure 6) and temperature (Figure 7) in different HF/HNO_3 solutions [Österdahl and Rasmuson (II), 2006]. Even though the crystal growth rate increases with increasing temperature, temperatures above approximately 60°C are not desirable due to the increased corrosion and waste gas problems at higher temperatures. The supersaturation is limited by an increased risk of scale formation at high supersaturation. The supersaturation in the crystalliser at steady state depends on the flow rate, the supersaturation of the incoming solution and the crystal surface area available for growth in the crystalliser. Some scale formation was observed in the pilot crystallisation experiments. The scaling only occurred in stagnant zones. The probability of scale formation at high supersaturation levels must be further evaluated in the actual equipment (or similar in size, materials and construction).

3.3 Membrane filtration in pilot scale

The pilot experiments included two membranes. In this equipment the membranes are working in a similar way as in a full scale membrane plant. The membranes studied were two spiral wound membranes, MP34 from Koch, and NadirOY, NP030 from Microdyn-Nadir. A number of experiments have been performed with the pilot scale equipment. The range of metal concentration in these experiments can be found in Appendix 2 Nanofiltration pilot experiments.

3.3.1.1 Test conditions

First the pickle liquor was filtrated by microfiltration to remove particles that otherwise would clog the nanofiltration membrane. The filtrate is passed to a storage vessel where the solution is heated to a temperature in the range of 45 to 50 °C. The warm solution is then pumped to a feed and working tank from where it was transported to the membrane module using a high pressure pump. The membrane module consisted of a 2.5 inches spiral wound nanofiltration membrane. The permeate stream leaving the nanofiltration unit with a low metal content was removed from the system to a storage tank. The retentate stream is led back to the feed tank. The retentate stream could thus be circulated several times through the nanofiltration module until a desired metal concentration is reached. For continuous operation the retentate stream could also be split off to a separate storage vessel. The retentate solution was transported at a desired rate (1 to 4 L/h) to a 10 L scale crystallisation vessel using a peristaltic pump.

The permeate flux (flow per time and area) was studied as a function of pressure, temperature, metal-concentrations and running time.

Two different acids were studied:

1) OKS Avesta KBR with an original composition of 22.6 g/l metal, HF 2.9 M and HNO_3 2.8 M, analysis by OKS
2) SMT Stainless steel with an original composition of 23.7 g/l metal, HF 2.0 M and HNO_3 2.7 M, analysis by IVL

For each acid several experiments were performed where the acid was concentrated about 2 times (VRF 2).

3.3.1.2 Results and discussion

The effect of pressure and temperature were only tested for one membrane. It was supposed that similar results would be achieved with the other membrane.

MP34 membrane

Effect of pressure

The flux was tested at different pressures with acid from OKS, see Figure 14 below.

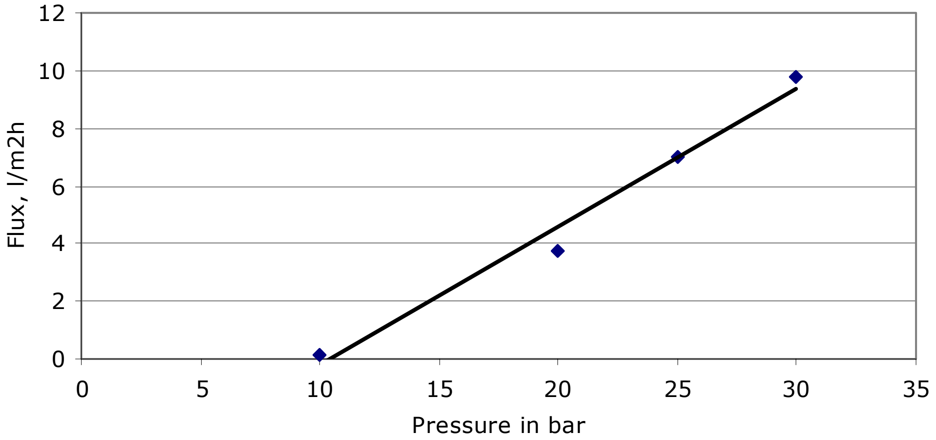

Figure 14 Increase of flux with increased pressure for a pickling acid solution with a metal content of 22.5 g7l. Concentration of HF is 2.9 M and HNO_3 2.8 M.

At a pressure of 10 bar the flux is almost zero. The flux increases steadily with increased pressure. By for example, increasing the pressure from 25 to 30 bars, the flux increases from 7 to 10 l/m^2h. Long time effects of different pressures on the flux were not studied.

The maximum working pressure recommended for this membrane is 35 bars at the tested temperature of 45°C.

Effect of temperature

The maximum operation temperature was 45 °C. It is known that the flux usually increases with temperature, a typical order is 30 % increase by 10 °C. On the other hand it is needed to lower the maximum operational pressure when operating the membrane at higher temperatures. As the pickling bath and the crystallisation step are preferably operated at higher temperatures it was chosen to operate the nanofiltration at temperatures around 40 to 45 °C

Effect of metal concentration

The experiments show clearly that the flux is depended on the metal concentration. In Figure 15 the average for experiments 2-14 is shown. A possible explanation for the variation between the different experiments is the variation in pressure and temperature, even if they were in the range of 5°C and 3 bar.

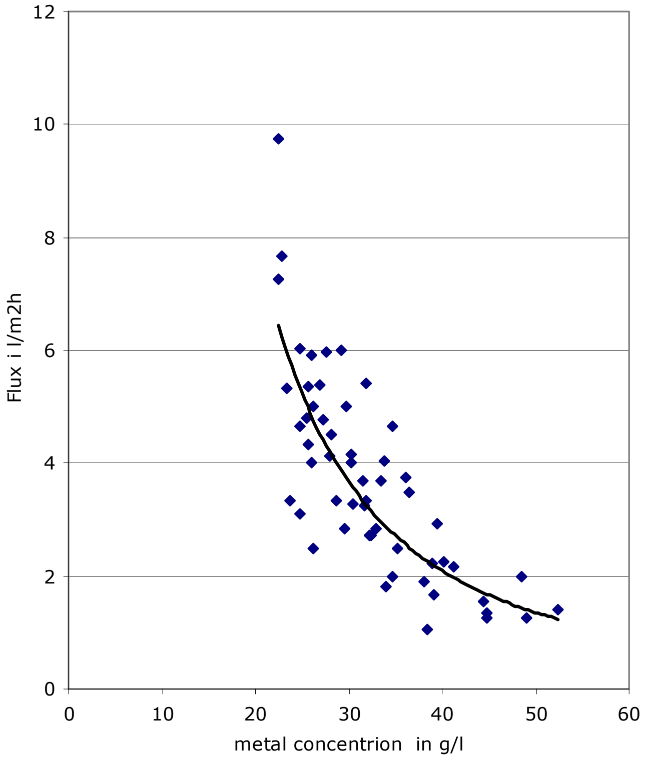

Figure 15 Flux against metal concentration for MPS34 pilot membrane, results from 13 experiment included. Pressure is varying between 30 – 33 bar, temperature between 40 –45 °C.

The influence on flux of increased contents of nickel was also investigated by adding nickel nitrate. This is important due to the higher nickel solubility compared to iron and chromium.

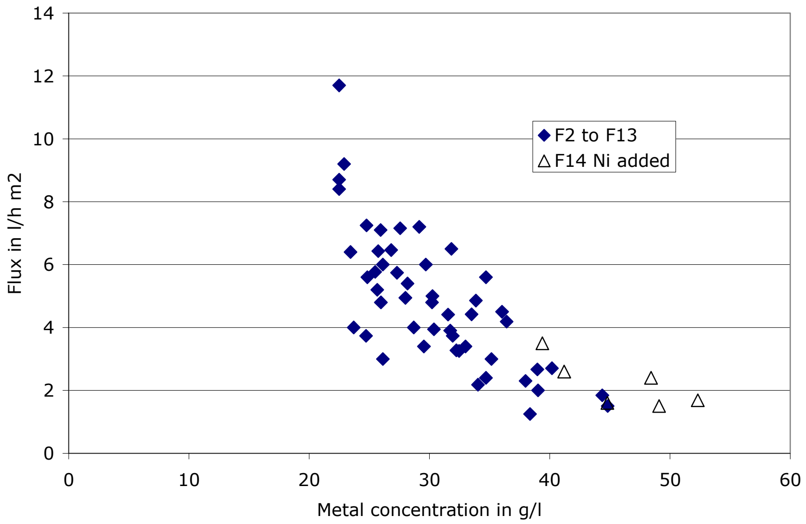

Figure 16 Flux against metal concentration for MPS34 pilot membrane compared with experiment 14 (triangles) where approximately 6 g/l Ni was added to a total concentration of initial 10 g/l. After up concentrating the nickel concentration was 14 g/l.

When comparing the flux for the experiments where the nickel is added the reduction of flux by increasing metal in experiment 14 is similar as the other experiments where nickel concentrations varies between 4-8 g/l. It seems that the flux reduction is depended on the total metal concentration in the acid solution in a similar way.

Effect of acid composition

When comparing all the data for the two different acids, no significant difference in flux at similar metal concentrations could be observed, see figure below.

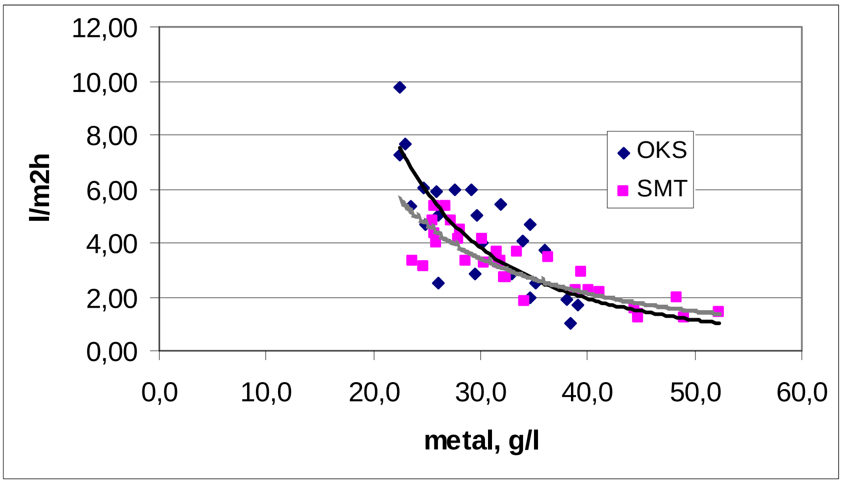

Figure 17 Comparison of flux versus metal concentration for two different acid, one from OKS (HF 2.9 M and HNO_3 2.8 M), and one from SMT (HF 2.0 M and HNO_3 2.7 M).

The figure above shows that the difference between the two acids is negligible under the tested conditions. Measurements of the acid concentrations before and after filtrations show no retention of the acids.

Effect of running time

With a total running time of 40 hours for the 15 concentration experiments, no time effect was noticed for the flux, with one exception. The first run showed a higher flux.

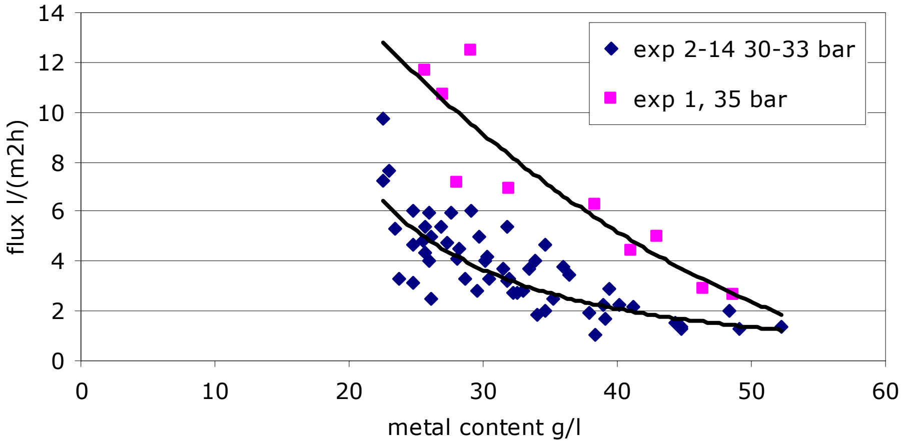

Figure 18 Comparison of the flux in the first experiment with a new membrane with the experiments 2-15 made with the same membrane thereafter.

A marked decrease in flux is noticed between the first run and the following. This effect could be caused by a deposition or by some change in the membrane at the first run, for example swelling of the membrane. There is a small difference in pressure. The first investigated experiment was performed at 35 bar, the following at pressures between 30-35 bar. This small pressure difference cannot alone explain the significant differences in flux.

Retention for metals and for salt

The retention for NaCl was much higher than what the data sheet for the membrane declares; here 35 % retention for a 5 % NaCl solution at 30 bars and 30 °C was stated. Our measurements for this membrane gives a show a much higher retention, see Table 11 below.

Table 11 Retention of NaCl solutions for MPS34 membrane

Date	Descr.	Temp. °C	Pressure bar	NaCl g/l	Flow Water l/h	Flow NaCl l/h	Cond. Conc.	Cond. Perm.	Retention. %
03-feb	After F1	29	35	1.5	42	41	4200	2100	50.0
15-feb		26	33	5	47	42	9400	1500	84.0
17-feb	After NaOH	29	33	5		39	9130	1160	87.3
09-mar	After F5	29	33	5	38	35	9000	3200	64.4
24-mar	After F7	29	33	5	35	33	9200	4580	50.2
03-maj	After F11	29	33	5	38	37	9500	6900	27.4
04-maj	After F13	29	33	4	40	35	7500	1500	80.0
08-jun		29	33	4	40	36	6900	1220	82.3

The retention for NaCl varies between 50 and 84 %, with exception of one value. No decrease in retention was observed between February and June, the total running time was 40 hours.

By measurements with Scanacon and Dr Lange the analyses showed that the retention of iron, chromium and nickel were more than 90 % in total in experiments 2-13. The inlet concentrations of the metals were here approximately 15 g/l for iron, 2 g/l for chromium and 5 g/l for nickel.

The retention of nickel in experiment 14, where the nickel concentration was increased to 14 g/l, was, as well, more than 90 %.

For experiment F10 the analysis was complemented with ICP metal analysis for the SMT acid.

Table 12. Metal analysis for experiment F10, MP34 membrane, concentrations in g/l.

Iron concentration		Chromium concentration		Nickel concentration	
Concentrate	Total permeate	Concentrate	Total permeate	Concentrate	Total permeate
62	3.2	5.4	0.26	5.6	0.34

Nadir membrane

One additional test with a Nadir Spiral membrane with a total area of 1.8 m^2 was also performed at 40 bar pressure and 49.5°C. In table below is the flux at two different concentrations shown. The investigated acid was an acid from OKS at Avesta with an acid concentration of 2.4 M HF, and 2.5 M HNO_3 according to analysis from OKS.

Table 13. Flux for Nadir membrane at two different metal concentrations. Metal concentrations as result of Scanacon analysis and sum of chemical analysis of Fe, Cr, Ni, Mo.

Metal (Scanacon), g/l	Metals (chemical) g/l	Flux, l/m^{2}h
26.4	47.4	48.9
35	58	43.3

There is a significant difference in this case between the metal results from the Scanacon analysis and the chemical analysis. As the Scanacon analysis is based on density measurement and calculations from acid concentrations, the values are more uncertain than the values from the chemical analysis. In earlier investigations, there was not a large difference between the chemical and Scanacon analysis. Independently which metal values are valid, the results show that the permeate flux remains high during the concentration period.

Table 14. Metal concentrations in g/l of iron, chromium and nickel at feed and permeate side for VRF1 and VRF2.

	Fe_{feed}	$Fe_{perm.}$	% Fe retention	Cr_{feed}	$Cr_{perm.}$	% Cr ret. retention	Ni_{feed}	Ni_{perm}.	% Ni retention
VRF1	32	20.2	37	5.4	3.3	39	8.9	5.8	35
VRF2	40.8	25	39	6.9	4	42	9.3	6.8	31

The retention for these analysed metals is about 30-40 per cent both at the start and the end of the concentration.

The lower metal retention compared to the MP membrane might be compensated by the higher flux for this membrane.

The retention of this membrane is much lower than the retention for the MP34 membrane, but the flux is much higher. When comparing the flux at 47 g/l with the MP34 membrane for the same concentration (see Figure 5) it can be noticed that the flux that is approximately 40 times higher. This means that even if the retention is significantly lower the total metal separation per square meter will be higher for this membrane. This has been further investigated in the simulation of the system.

3.4 Method for on-line concentration measurement

On-line measurement of acid and metal concentrations has not been investigated specifically in this project, but was part of a parallel project. On-line measurement of the concentrations can be used to efficiently control a full-scale process for acid and metal recovery with hybrid technology.

A technology that can be used for online measurements is based on acoustic emission from turbulent flow. Characterisation of a fluid with advanced acoustic leads to spectra that are assumed to be unique or at least give a diagnostic picture of the characteristics of the fluid. Such system, including suitable signal processing and using multivariate calibration makes it possible to trace the desired parameters. Characterisation of a pickling acid fluid with acoustic measurements is based on a number of steps according to Figure 19.

The physical phenomenon that generates vibrations, i.e. the acoustic signal, is turbulence that is created by letting the process liquor flow pass through a constriction in a pipe. This is usually accomplished by a circulation loop that is connected to the process and returns the process liquor to the process after the measurement. Many physical parameters influence the turbulence and thus the signal, such as phase distribution, particle size, emulsion size distribution, viscosity and density of the different phases etc. These are related also to the chemical characteristics of the fluid, which means that the measured signal contains information about both physical and chemical properties of the process liquor.

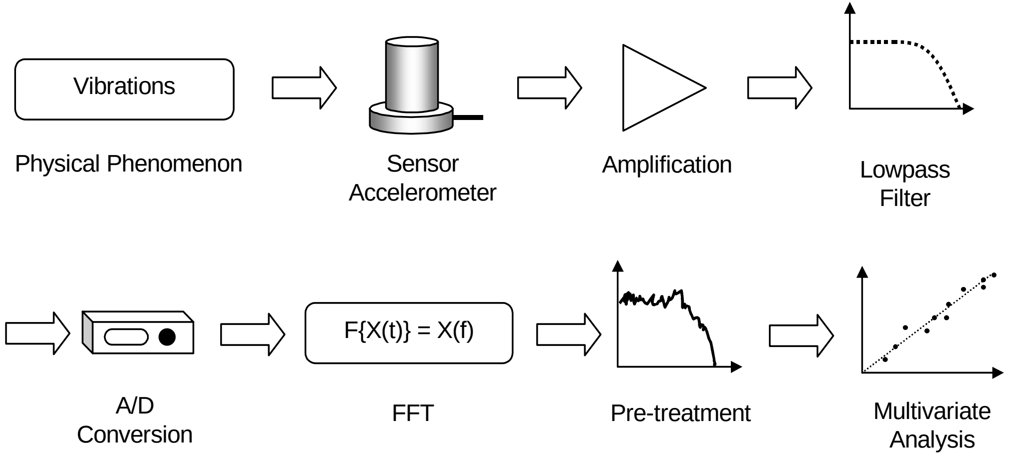

Figure 19. Schematic of steps in acoustic measurements.

In a project parallel to this study IVL has built an acoustic chemometric equipment especially for mixed acids. It is made of materials that would sustain the hash acids. The equipment has been tested in the laboratory with initial promising results. The equipment was built from start to work as laboratory equipment or in a pilot plant or industrial plant. Except for the control logic for the equipment and a casing for the measurement and control computer the equipment is ready for use in an industrial plant. The equipment can be used for tests in a bypass to the pilot plant or a full-scale plant.

4 Design and simulation of a full scale-reactor

In order to predict the effect of a full-scale cleaning system on the pickling acid system a mathematical model of the system based on mass balance on each following bath was developed. With this model it is possible to follow the changes of concentration over time in the bath after a change of one inlet stream. Also the steady state concentrations will be result of the model. The model is illustrated in Figure 20 . More details about the model are provided in Appendix 3.

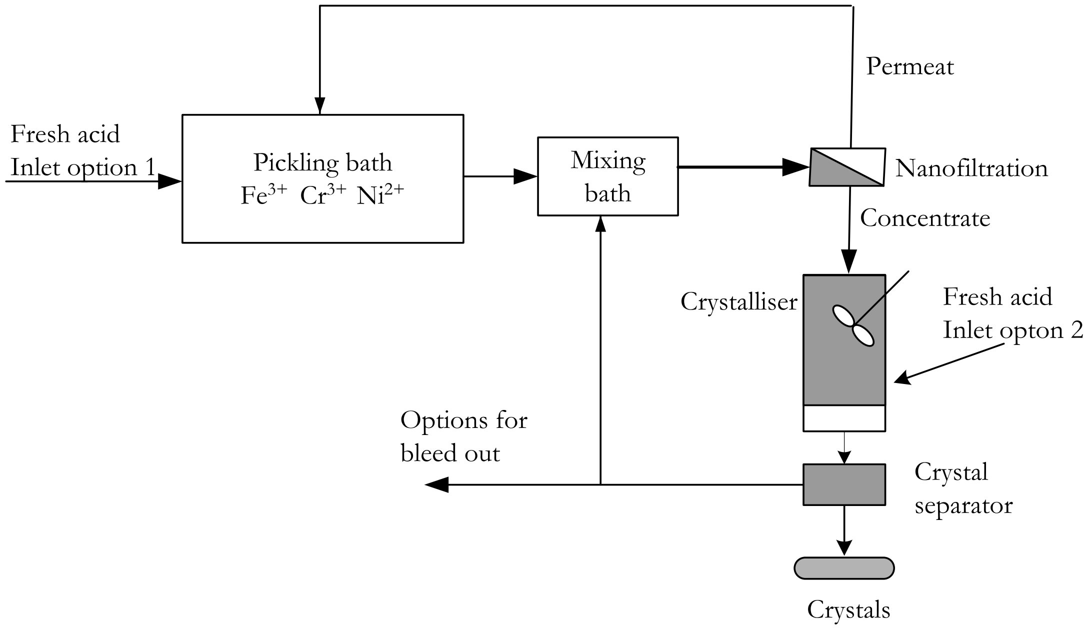

Figure 20. Process scheme for simulation of the hybrid system.

Inlet data of the model were the concentrations of the acids and the size of crystallisation and membrane units. Flow rates into the membrane and amount liquid “blooded” out from the system are important factors, which influence the total performance. The bleeding is necessary to keep the amount of nickel at a sufficiently low concentration, as high total metal contents effect the membrane capacity negatively.

A mass balance of the acids gives that for HF : $V_{in} * c_{in\text{-}HF} = Cryst * c_{cryst\text{-}HF} + V_{out} * c_{out\text{-}HF}$

The HF in the crystals is mainly in form of metal fluorides. The inlet for acid can either be situated in the pickling bath or elsewhere, for example in the crystallisation unit itself. The advantage with an addition in the crystallisation bath would be an increased HF concentration in the crystalliser, which favours the crystallisation. A disadvantage could be a more difficult process control of the bath, as the acid is not added directly into the pickling bath. Also an additional loss of acid can be expected when bleeding-out.

The mass balance for HNO_3: $V_{in} * c_{in\text{-}HNO3} = Cryst*c_{cryst\text{-}HNO3} + V_{out} * c_{out\text{-}HNO3}$

Mass balance for metals: Dissolved metals = $Cryst*c_{metals} + V_{out} * c_{out\text{-}metals}$

The metals are dissolved during the pickling of the stainless steel goods in the pickling process. The mass balance is valid for all metals present in the bath.

Amore detailed mass balance over all the steps are described in Appendix 1.

Concentration of metals in the different bath

High concentration of nickel in the bath will be reached with no bleed out of acid. The basis for this is the high nickel saturation concentration, which is needed to reach crystallisation. At the moment there are no exact figures for these concentrations available, but measurements in this project show that the saturation concentration is higher than 20 g/l. Thus, it was assumed that crystallisation begins at a concentration of 35 g/l, based on earlier IVL work.

Because of need of supersaturation for crystallisation of nickel, the final concentration could be as high as 45 g/l of according to our assumptions. A similar assumption is that the concentration to reach crystallisation will be 6 g/l for chromium.

High nickel concentrations cause a low flux for nanofiltration permeates at higher concentrations. To avoid the flux getting too low it is therefore probably necessary to bleed out some of the acids. The disadvantage with out bleeding is that acid has to be treated in the neutralisation plant.

4.1 Results of the simulations

The design of the treatment system for pickling baths includes two cases, one at SMT AB and one for OKS in Avesta. The background data for these two cases are presented in Appendix 5.

It is important to state that the simulation can be further improved by changing the values of different parameters. In order to get the optimal configuration from an economical and environmental point of view more information is needed, e.g. about the life-time of the equipment and long time average performance.

In SMT the pickling bath studied can dissolve 8 kg of metal each hour. The average concentration of acids is 2.3 M for HNO_3 and 1.75 M for HF. Today this unit produces per year 2150 m^3 wasted pickling acid that has to be treated and disposed off. The temperature in the bath is 45 °C.

In OKS Avesta the pickling bath can dissolve approximately 80 kg metals per hour. The temperature in the bath is between 55 and 60 °C. Average concentrations of acids are 3 M HNO_3 and 3 M HF. For the OKS Avesta case today approximately 32 000 m^3 wasted pickling acid per year has to be treated and land disposed.

For each case, simulations with the two promising membranes that are different in retention and flux, have been performed. The annual running time is estimated to be 8000 hours

Table 15 Simulated systems at steady-state for 4 cases.

	Membrane type	MP34 Case SMT	Nadir Case SMT	MP34 Case OKS	Nadir Case OKS
	Amount m^3 pickling without recovery	2156	2156	32000	32000
	% reduction of Acid volume	90%	86%	98%	98%
Inlet data	Size of Pickling bath. m^3	3.84	3.84	37.33	37.33
	Size of mixing bath	2.00	2.00	20.00	20.00
	Size of Crystalliser. m^3	4.00	6.00	55.00	50.00
	Magma-density for crystalliser. weight %	15.00	15.00	15.00	15.00
	Membrane area in 1000 square meter	0.36	0.055	4.30	0.60
	Inlet flow into membrane m^3/h	1.80	5.00	18.00	45.00
	Out bleeding. m^3/h	0.026	0.038	0.072	0.072
	Out bleeding. m^3/annual	212	302	575	574
	Retention of metals	0.90	0.40	0.90	0.40
Calculated system conditions	Permeate-flow. m^3/h	0.35	1.87	4.14	16.12
	Iron-content in pickling bath. g/l	19.53	19.51	15.58	14.62
	Metal content in pickling bath. g/l	29.10	36.14	25.26	43.52
	Metal content in mixing bath	53.99	45.23	53.07	55.34
	Metal content in concentrate. g/l	65.45	53.18	66.90	64.60
	Supersaturation Fe in crystalliser. c/c*	1.41	1.32	1.36	1.38

In Appendix 5 the outlet parameters for the systems described more in detail.

SMT cases:

The critical iron concentration to avoid crystallisation in the pickling bath is calculated to be 19.7 g/l. In order to keep the concentration below this concentration 360 m^2 MP34 or 55 m^2 Nadir membranes are used. The flows into the membranes are estimated to be 1.8 for the MP34 respectively 5 m^3/h for the Nadir case. The size of the crystallisers were chosen to be 4 respectively 6 m^3.

To not avoid too large membrane areas a bleed out of pickling acid from the circulating system was included in the calculations. Without out bleeding high concentrations of nickel at 40 g/l could be expected, which will decrease the flux substantially. With the bleeding proposed above the nickel concentrations in concentrate can be kept at below 25 g/l (see Appendix 5).

OKS cases:

Here the critical iron concentration to avoid crystallisation in the pickling bath is 15.5 g/l. The lower concentration is due to higher acid concentrations and also due to a higher temperature in the pickling bath compared with the SMT case.

A membrane area of 4300 m^2 MP34 or 600 Nadir membranes have been chosen. The crystallisation unit is 50 to 55 m^3 for both membranes. The inlet flow to the membranes is 18 for the MP34 membranes and 45 m^3/h for Nadir.

The bleed out is proportionally lower in the OKS cases, which results in a higher nickel concentration in the concentrate, 38 g/l. For a higher bleed out, as for the SMT cases, it could be possible to work at lower nickel concentrations, and thus use less membrane area, approximately 2800 m^2 for the MP34 case 400 m^2 for the Nadir case. The reason for choosing less bleed out in the OKS case was to keep down the amount of acids going out from the system below the stated effluents today.

4.1.1 Mass balances

As result of the simulation, mass balances for the nitric and hydrofluoric acid as well as for iron, chromium and nickel were established. Figure 21 and Figure 22 illustrate the mass balance for SMT in one case. The mass balances for all the studied cases are shown in Appendix 8.

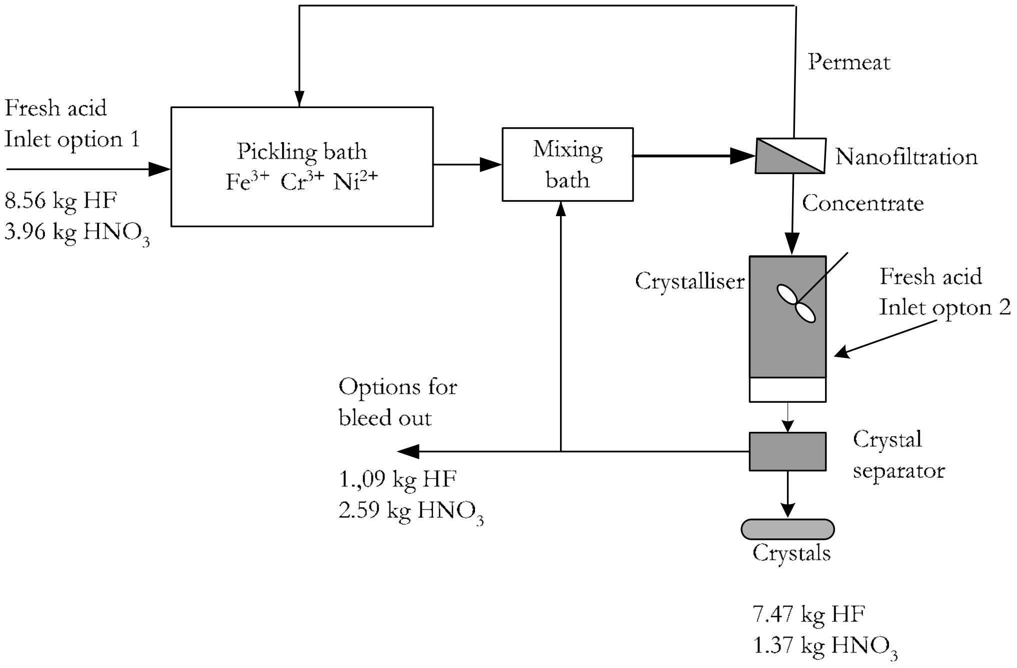

Figure 21 Acid balance in acid per hour for circulated pickling bath, in MP34 membrane SMT case.

The added acid in this case should be compared with the added acid without recirculation, 323 ton HNO_3 and 110 ton HF (Appendix 4) annual or 40 kg HNO_3 and 13.8 kg HF per hour.

The reduction of used HNO_3 is thus 90 % and the reduction of HF is 40 %. Most of the used HF in recirculation system goes to the produced crystals. If these crystals are treated further to separate hydrofluoric acid and metals, the total regain of HF could be as high as the HNO_3 regain.

In Figure 22 below is the balance for metals shown.

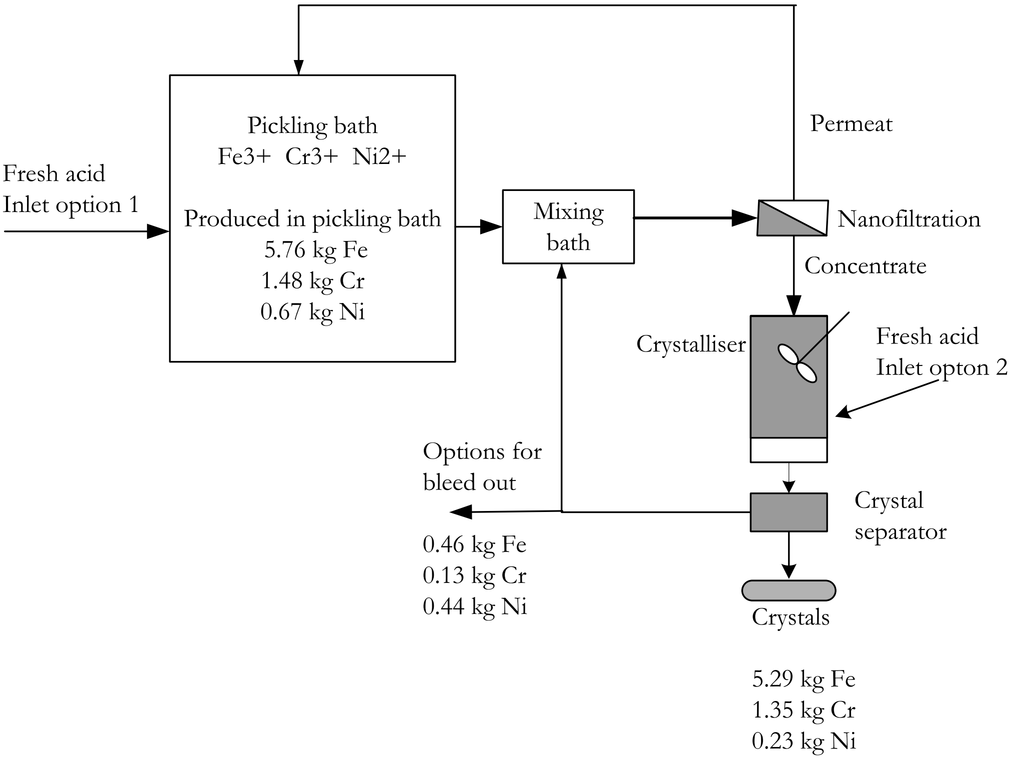

Figure 22 Metal balance in metals per hour for circulated pickling bath, in MP34 membrane SMT case.

Almost all of the dissolved chromium and iron could be found in the crystals. For the nickel approximately 60 % will be found in the crystals.

5 Energy demand and potential energy gains for the hybrid system

The energy balance and economics of the treatment with the hybrid treatment system was compared with a system with acid retardation, neutralisation and landfilling, which is a common treatment today. Values were calculated for two cases and with two different membranes. The calculations do not include the energy demand or savings for treatment of the crystal fraction, e.g. for thermal treatment, but they take into account the part of the chemicals that are saved or reused on site.

The operation of the hybrid system implies an energy demand for pumps and impellers. A part of this energy can be reused for heating the pickling baths. When using heat exchangers theoretically almost all energy converted to heat in the hybrid system could be regained. Besides, less energy is needed to heat up the acids, because less fresh acid will be added due to the recycling from the hybrid system. The possibility to save energy for heating depends on the situation at each site. If excess heat already is available, there is still a possible saving, but the heat energy can not be used directly at the production site.

The energy saving by using the treatment system is mainly due to reduced energy demand in the production of chemicals such as hydrofluoric acid. There will also be directly lowered energy consumption in the neutralisation step, because less acid has to be treated. Energy today used for acid retardation, mainly pump energy, is not needed with the hybrid system.

The estimated energy demand and savings when using the hybrid system are listed in the following table for the four simulated cases.

Table 16 Energy demand in kWh annual

Basic data	MP34 SMT	Nadir SMT	MP34 OKS	Nadir OKS
Crystallisation (m^3)	4	6	55	50
Membrane (m^2)	360	55	4300	600
reduced amount new pickling bath	90%	86%	98%	98%
Energy balance	kWh	kWh	kWh	kWh
Energy used for treatment system	88 000	126 000	1 216 000	1 400 000
Energy savings				
lime	1 290 000	1 230 000	8 380 000	8 360 000
HF	291 000	237 000	361 000	321 000
HNO_3	1 102 000	1 051 000	6 480 000	6 480 000
operation treatment plant	7 500	7 500	15 000	15 000
reduced energy need for heating pickling bath	79 000	76 000	1 460 000	897 000
reduced energy need for acid retardation	4 300	4 300	64 000	64 000
Total savings kWh annual	2 690 000	2 480 000	15 500 000	14 700 000

The energy balance results in savings for all investigated cases. The largest part of the savings is derived from the reduced use of chemicals. The energy saved can be 20-30 times larger than the energy needed for the operation of the hybrid equipment, i.e. not including the treatment of crystals for metal and fluoride recovery, which probably uses more energy than can be saved. There are also direct savings at the steel site possible, due to reduced demand for heating of fresh acid, no acid retardation and reduced use of the neutralisation unit.

The direct savings potential at the steel industry sites is in the same order of magnitude as the energy used for the hybrid system. Savings can be gained by for lowered energy demand to heat pickling bath, no need to run acid retardation and less energy demand in the neutralisation step. Actual savings depend on the possibility to reduce the energy in proportion to the reduced demand for operation of the different units. The neutralisation plant for example will still be needed for treatment of rinse waters. To reduce the operation of the neutralisation step in proportion for the reduced need due to the hybrid system, investments in the neutralisation step might be necessary.

Crystallisation unit

The energy demand is estimated to be 0.8 kW per m^3 crystalliser volume. This energy is needed to run the impeller. No energy is needed for heating of the crystalliser, because the walls are heat-isolated. This gives a total energy of 3.2., 3.8, 40 and 44 kW for the chosen crystallisation of 4, 6, 50 and 55 m^3 respectably.

Microfiltration

The flow into the nanofilter must be pre-treated with a microfilter. The chosen microfilter was delivered by Scanacon. The required pump effect for this filter is 1 kW per m^3 and hour.

The high energy demand is caused by a high circular flow used in order to have a sufficient cross flow in the tubular membranes.

For the OKS case, for instance, the inlet flow into the MP34 is 18 m^3, therefore the needed effect will be 18 kW. Correspondingly for the Nadir system the inlet flow is 45 m^3 and consequentially the effect used 45kW. In the SMT case the energy need will be 1.8 kW (MP 34) and 5 kW (Nadir).

Nanofiltration

In the nanofiltration step, energy is needed for establishing the flow rate and to reaching the pressure used for the filtration, 35-40 bars, as well as the pressure drop for the filter, which is in the order of 1- 3 bar.

The inlet flow for the OKS case is varying between 18 m^3/h for MP34 and 45 m^3/h for the Nadir case. The pressure drop is higher for the larger membrane area. The energy demand is estimated to be 90 kW for both membrane systems. For the SMT case the energy effect is estimated to be 6 kW.

Energy saved in the neutralisation plant

Without the hybrid system, a larger neutralisation plant is needed, which in OKS case is estimated to have a storage tank with 100 m^3 volume, a reactor tank with 2 m^3 volume (based on half hour residential time) and a sedimentation tank of 6 m^3 (1.5 hours residential time). For SMT the size s will be 20 m^3 storage tank, 1 m^3 reactor tank, and 2 m^3 sedimentation tank.

The energy consumption for such a unit is estimated to be 0.8 kW/m^3 for the stirred reactor tanks, i.e. 0.8 and 1.6 kW for the reactor tanks in the different cases. Energy for pumping between the tanks is estimated to be negligible.

With the hybrid system reducing the amount of pickling acid to be treated, a smaller neutralisation plant can be used, which means a correspondingly smaller energy use. If the amount of pickling acid dumped is reduced with 90 %, the annual energy savings are roughly estimated to be 1.6 kW*8000 (hours annually)*0.9 (reduced amount pickling acids) = 11 500 kWh for the OKS case. In practice, it will probably not be possible to reduce the operation of the neutralisation plant in correspondence to the reduced amount of pickling acid, which implies less energy saving.

Energy saved in the heating of the pickling bath

Theoretically all the used energy for micro filtration and nanofiltration, which is converted to heat, could be used for heating the pickling bath. But because the equipment works at somewhat lower temperatures in the membrane and crystallisation system, not all of this energy can be used. There is also a lower need to heat incoming acid when the hybrid system is used, because less fresh acid is used. If there is excess heat available as it is the case at some production sites, the reduced need for heating can not be used directly on the site to save energy.

Energy savings for the chemicals

The energy for producing 1 kg of chemical was calculated in an earlier work by IVL and OKS.

Table 17 Energy cost in kWh to produce one ton of a chemical

	GJ/ton
Nitric acid	13.6
Fluoric acid	33
Calcium-oxide	8.95

See Appendix 6 for more information.

There is a further potential to recycle chemicals and metals by treatment of the crystals, for instance FeF_3 to hydrofluoric acid and metals ready for re-use. For the SMT case approximately 60 ton of HF could be recovered. In OKS Nyby approximately 600 ton of HF could be regained this way. There will also be an energy demand for this treatment, which is probably higher than the savings from the recycling of chemicals from this part of treatment.

6 Preliminary costs and savings estimations for a hybrid system

The estimations of cost and savings are based on the results of the pilot scale experiments. As only a few experiments have been performed and number of uncertainties exists, there are only rough estimations giving an impression on the order of magnitude of costs and savings but not giving exact data.

Several assumptions have been made for the estimations, like a total extra cost of 70 % for building the system and for a control system in addition to the equipment costs. The running cost differs between the cases due to different membrane areas required. A rough estimation is that that the membranes have to be exchanged two times a year. The actual life-time can be shorter or longer. The cost per square meter membrane is 1100 KSEK according to the suppliers.

The cost calculations do not include the costs for treatment of crystals, e.g. by thermal treatment. Neither are savings through recycling of metals and fluorides from the crystals included.

The personal costs are based on an estimation that one person has to work one to two hours per day with the recovery system. Energy costs are based on the energy calculation and a cost of 0.3 SEK/kWh. The pay off costs are based on a 20 % annual pay-off. Cost per kg saved chemical are based on figures from the involved companies.

Table 18 gives an impression of the economics for the hybrid system. The table consists of two parts. The costs for investment and operation of the hybrid system have been estimated for the different membranes at two production sites. The second part describes possible savings when installing the hybrid system, i.e. "annual savings" do not take the cost part into account.

Table 18 Economic estimations for 4 cases

Basic data	MP34 Case SMT	Nadir Case SMT	MP34 Case OKS	Nadir Case OKS
Crystallisation equipment	4	6	55	50
Membrane (m^2)	360	55	4300	600
Reduced amount pickling bath	90%	86%	98%	98%
Costs				
Investment costs				
Membrane equipment (micro +nanofiltration)	3 000 000	2 500 000	10 000 000	7 000 000
Costs for dewatering system for crystals	800 000	800 000	2 000 000	2 000 000
Crystallisation equipment	280 000	320 000	1 380 000	1 380 000
Additional costs (build. start-up ...)	2 856 000	2 534 000	9 366 000	7 266 000
Total investment costs	6 936 000	6 154 000	22 746 000	17 646 000
Operating costs (SEK/year)				
maintenance 1-2h /day	31 250	31 250	62 500	62 500
Membrane costs/year	792 000	121 000	9 460 000	1 320 000
Energy costs. Year	26 400	37 920	364 800	420 000
Pay-off costs	1 387 000	1 231 000	4 549 200	3 530 000
Annual costs	***2.2 MSEK***	***1.4 MSEK***	***14.4 MSEK***	***5.3 MSEK***
Savings by recycling				
Lime	570 000	543 000	3 700 000	3700000
HF	235 000	191 000	307 000	273 000
HNO_3	481 000	459 000	2 607 000	2 607 000
treatment plant (precipitation)	1 787 000	1 704 000	400 000	400 000
landfilling fee	300 KSEK to 1.5 MSEK	290 KSEK to 1.4 MSEK	2 MSEK to 10.3 MSEK	2 MSEK to 10.3 MSEK
need for heat in pickling bath	23 900	22 700	437 000	269 000
Need for energy in acid retardation	1 300	1 300	19 200	19 200
Annual savings	**3.4 to 4.6 MSEK**	**3.2 to 4.4 MSEK**	**9.5 to 17.7 MSEK**	**9.3to 17.5 SEK**

Landfilling Today both sites have internal land disposal. But this will probably not be allowed in the future. A cost of 200 SEK/ton for internal landfilling and the higher cost for external landfilling of 1000 SEK/ton were used for calculation.

Precipitation cost For SMT case calculated the total cost per kmol acid 250 SEK was used, which according to SMT should include piping costs, precipitation, chemicals and electricity. (The calcium oxide cost was subtracted from this value, because these costs were calculated separately in our study). In OKS only the capital and energy cost for the precipitation unit were used, based on a total cost of 2 MSEK (100 m^3 storage tank , 8 m^3 reactor tank and 20 m^3 sedimentation tank) and 400 000 annual pay-off in the OKS case for the precipitation tank.

Table 19. Costs for chemicals and landfilling in SEK/kg

	SMT	OKS
Lime, SEK per ton	1 100	1 100
HNO_3, SEK per ton	1 650	1 520
HF, SEK per ton	7 400	7 800
land disposal internal costs SEK per ton	200	200
land disposal external costs SEK per ton	1 000	1 000
Energy cost SEK/kWh	0.3	0.3

The OKS case: The investment costs for the membrane system including micro filter are estimated to be 7-10 MSEK. Compared to conventional membranes systems a more corrosive environment results in a higher price. The costs for the crystallisation unit are estimated to be 1.38 MSEK. The costs for the crystallisation unit are specified more in detail in Appendix 7. Besides, there is the cost for a filter press of 2 MSEK to reduce the acid concentration in the crystals.

Total investments cost are thus estimated to be 17.6 to 22.7 MSEK.

The annual costs: It is obvious that the membrane costs are a high for the MP34 case, approximately equal to the pay-off costs for the equipment. The membrane costs are substantially lower for the Nadir membrane. The annual membrane costs depend highly on the membrane life-time, which only has been estimated for both membranes. Maintenance and energy cost are comparatively low. The pay-off costs based on amount metal treated are 7 KSEK per ton treated metal for the MP34 system and 5.5 KSEK for the Nadir system. The total costs per ton treated metal (including membrane, maintenance and energy costs) are 22.4 KSEK for the MP34-system and 8 KSEK for the Nadir system.

The annual savings: The savings for chemical costs and savings for land disposal costs (external) are both in the order of 6 MSEK annual. Energy savings at the site are comparatively low.

The SMT case: The investment costs for the membranes and crystallisation are lower because smaller units are needed, the total investments costs are estimated to 1.4 to 2.2 MSEK.

The annual costs: Also in this case the MP34 membranes are more expensive than the Nadir-membranes, because more membrane area is needed. The annual membrane costs depend highly on the membrane life-time here as well. The pay-off costs are higher in the SMT case, if based on amount metal treated.

Annual savings: The savings are lower than in the OKS case in the same way as the investment costs. The reason for this are the proportionally higher costs for the hybrid equipment.

7 Conclusions and recommendations for future work

The project included laboratory experiments as well as a short period of pilot plant experiments. The recommendations are based on the results from these experiments

7.1 Findings from the project

Within the project, new information about the crystallisation of iron fluoride in pickling acid was found by experiments. Solubility and growth rate data support the design of an efficient crystallisation step. Solubility relationships suggest that it would be beneficial to add the make-up acid to the pickling process already in the crystalliser [Österdahl et al., 2006]. The temperature in the crystalliser should be kept high to increase the crystal growth rate. A supersaturation of 1.4 – 1.8 in terms of iron content in the crystalliser works well and does not give rise to scale formation according to pilot plant experiments at 40- 50°.

The membrane experiments indicate that two membranes can be used for the nanofiltration step: MP 34 from Koch and NadirOY NP030 from Microdyn-Nadir. The Koch membrane has a higher metal retention, but a lower flux and vice versa for the Nadir membrane. At the moment, there are only lab-scale experiments investigating the life-time of the membranes.

The project results indicate that hybrid technique can be an alternative solution that has a number of advantages as: reduced waste processing, saved chemical costs and reduced environmental impact at landfilling sites and downstream water-treatment. Simulations of the combined process indicate that it is possible to use the combination of nanofiltration and crystallisation for the continuous removal of excess metals from the pickling process. It might be necessary, though, to bleed out some acid in order to avoid high nickel concentrations.

Energy calculations show that the implementation of the hybrid technique allows saving energy. The main savings are due to the reduced consumption of chemicals, which partly have a relatively high "energy burden".

7.2 Future work

The project demonstrated that the hybrid system can achieve the wanted metal separation that will allow acid recycling. There are still some issues that could not be fully addressed in this project. One important question is the durability and life-time of the equipment, like for the membranes as mentioned above. Pilot plant experiments at the steel industries for a longer time would allow getting more information about the life-time of the membranes and the reliability of the hybrid system during a longer time. The project did not investigate if continuous or batch wise operation is preferable in a full-scale application. Batch wise operation can lead to a larger risk for clogging of equipment due to crystallisation at longer residence time e.g. between charges. A batch process gives on the other hand the opportunity to re-dissolve scaling that was formed in the previous batch.

The preliminary cost estimations indicate that it is favourable to run a larger hybrid system compared to smaller solutions. A bleed out of maybe 10 per cent of the total acid might be necessary in order to maintain a nickel concentration that does not lower the efficiency significantly. Also this is a question to be investigated during longer experiments.
In a pickling plant with recovery and recirculation the concentrations of various compounds like Nickel, Chromium and Molybdenium will build up to levels higher than those of todays spent pickle bath solutions. Hence, it is necessary to further explore the influence of these compounds on the crystallisation of b-FeF3Pts3H2O and determine in what form they themselves may crystallise.

Accordingly also the solubility and crystallisation of these solids in the prevailing solutions needs to be explored. Further work in the pilot plant and on scaling-up is also recommended

In addition to the investigated hybrid solution it will also be necessary to treat the crystals for recovery of acids and metal oxides. Such techniques are today commercially available and could be adapted to be used for the gained metal fluoride crystals, which would be part of the future work.. Such a system would then allow recycling the nitric acid and parts of the hydrofluoric acid directly. After thermal treatment the metals could be recycled as metal oxides and fluorides can be converted to hydrofluoric acid, thus allowing operating as an almost closed process.

8 References

Chupas, P.J., D.R. Corbin, V.N.M. Rao, J.C. Hanson and C.P. Grey, A Combined Solid-State NMR and Diffraction Study of the Structures and Acidity of Fluorinated Aluminas: Implications for Catalysis, J. Phys. Chem. B, 2003, Vol. 107, No. 33

Dézsi, I.; Pannaparayil, T.; Mulay, L. N., Magnetic ordering in dimorphic phases of $FeF_3 \cdot 3H_2O$: Magnetic and Mössbauer studies, *J. Appl. Phys.*, **1987**, 61(8), p 4346

Fernando, L. A., Solution Chemistry of HNO_3/HNO_3 Pickle Mixtures, Metallurgical Transactions B, 1990, 21B, pp 5-9

Fortkamp, U., K. Tjus and Å. Jansson, 2002, Avskiljning av metallfluorider vid blandsyrabetning – ökad förståelse av kemiska processer och framtagande av separationsmetoder, Institutet för vatten- och luftvårdsforskning, IVL, rapport nr B1441, IVL Swedish Environmental Research Institute. (in Swedish)

Fortkamp, U., S. Filipsson, K. Tjus, J.-E. Bjurhem and Ö. Ekengren, 2003, Factors influencing crystallisation from mixed acid pickling baths for stainless steel, IVL report nr B1519, IVL Swedish Environmental Research Institute

Karraker, D. G.; Smith, P K., 1992, α- and β-$FeF_3 \cdot 3H_2O$ Revisited: Crystal Structure and ^{57}Fe Mössbauer Spectra, *Inorg. Chem.*, **31**, pp. 1118-1120

Kreppler, A. Recovery of Nitric and Hydrofluoric acids from Pickling Solutions for Stainless Steel, Wire Industry, August 1978, p 639

Lentia GmbH, Chem. U. pharm. Erzeugnisse – Industriebedarf, 1969, Verfaren zur Herstellung von reinem Aluminiumfluorid, Bundesrepublik Deutschland, Offenlegungsschrift 1909948, 27-02-1969

Lentia GmbH, Chem. U. pharm. Erzeugnisse – Industriebedarf, 1974, Verfaren zur Kristallisation von Aluminiumfluorid- Trihydrat, Bundesrepublik Deutschland, Offenlegungsschrift 2313014, 15-03-1974

Macheteau, Y.; Charpin, P., 1972, Sur la decomposition thermique de FeF_3, 3 H_2O, *C. R. Acad. Sc. Paris*, t. **275**, (21 août), Série C

Nielsen, A.E., Electrolyte crystal growth mechanisms, Journal of crystal growth, 1984, 67, p 289

Österdahl, K.M. and Å.C. Rasmuson, Solubility of β-$FeF_3 \cdot 3H_2O$ in Mixtures of Nitric and Hydrofluoric Acid, J. Chem. Eng. Data, 2006, 51, pp 223- 229

Österdahl, K.M., 2005, Crystallisation of Iron Fluoride Trihydrate from Mixed Acid Solutions, Licentiate's Thesis, Royal Institute of Technology, Sweden

Österdahl, K.M., Å.C. Rasmuson, K. Tjus, U. Fortkamp, T. Schneiker and S. Åkesson, Precipitation of Iron Fluoride Trihydrate from Mixed Acid Pickle Liquors, Paper presented at the 45th International Conference of Metallurgists held in Conjunction with the 36th Annual Hydrometallurgy Meeting 1- 4 October 2006 in Montreal, Québec, Canada.

Österdahl, K., and Å. C. Rasmuson; Crystal growth kinetics of iron fluoride trihydrate, J Crystal Growth 296, 213-220 (2006)

Penfold, B. R.; Taylor, M. R. *Acta Crystallogr.* 1960, *13,* 953. A different diffraction pattern for FeF2.4H20 has been reported: *Os*teovskaya, T. V.; Amirova, S. A. *Russ. J. Inorg. Chem. (Engl. Trawl.)* 1969, *14,* 755.

Qiu, Y. and Å.C. Rasmuson, Crystal growth rate parameters from isothermal desupersaturation experiments, Chemical Engineering Science, 1991, 46(7), p 1659

Reddy, R. G., B. Chen, W. Wang, G. L. Horter and J. B. Stephenson, Solubility of Ni in spent pickling solutions, Minerals, Metals & Materials Society, 1991, p 801- 813

Silcoch, H., (Ed.), 1979, Solubility of inorganic and organic compounds, vol.3, Pergamon

Teufer, G., The crystal structure of β iron (III) trifluoride trihydrate, β-$FeF_3 \cdot 3H_2O$, Acta Cryst., 1964, 17, p 1480

Wang, S., 1992, Thermodynamic studies on HF-HNO_3-H_2O solutions containing Iron, Chromium and Nickel, Thesis for degree of Master of Science in Metallurgical Engineering, University of Nevada, Reno

Appendix 1. Data used for figure 3.

Solubility of β-$FeF_3 \cdot 3H_2O$ at 30°C,

Sample	*HNO_3 [mol/kg]**	*HF [mol/kg]**	*Fe (III) [g/kg]**
1a	0.0	1.8	28.1
1b	0.0	1.8	27.1
2a	0.9	0.9	21.6
2b	0.9	0.9	21.1
3a	1.0	1.9	17.3
3b	1.0	1.9	17.2
4a	1.0	5.8	12.9
4b	1.0	5.8	12.4
5a	1.9	0.9	18.4
5b	1.9	0.9	18.8
6a	1.9	1.4	15.4
6b	1.9	1.4	14.6
7a	1.9	1.9	12.6
7b	1.9	1.9	13.2
8a	2.0	2.4	11.0
8b	2.0	2.4	11.5
9a	2.0	2.9	10.3
9b	2.0	2.9	10.4
10a	2.0	3.9	8.6
10b	2.0	3.9	8.7
11b	2.0	5.9	7.9
12a	3.0	1.9	8.6
12b	3.0	1.9	8.1
13a	3.0	3.9	5.7
13b	3.0	3.9	5.5
14a	3.0	5.9	4.7
14b	3.0	5.9	4.7
15a	4.0	2.0	5.8
15b	4.0	2.0	6.2
16a	7.0	2.0	1.1
16b	7.0	2.0	1.1

* Expressed per kg solution, HF: free acid

For further information regarding these data see:
Österdahl, K.M. and Å. C. Rasmuson, Solubility of β-$FeF_3 \cdot 3H_2O$ in Mixtures of Nitric and Hydrofluoric Acid, J. Chem. Eng. Data, 2006, 51(1), pp 223- 229.

Appendix 2 Nanofiltration pilot experiments

Experiment	Start metal concentration mg/L	Final concentration mg/L
F1	23.0	48.7
F2	22.5	40.9
F3	22.5	39.0
F4	22.9	38.8
F5	27.5	38.4
F6	22.6	33.9
F7	22.6	33.0
F10	23.7	44.8
F11	23.7	31.9
F12	23.7	34.0
F13	23.7	40.2
F14	32.3	52.0

Appendix 3. Simulation of a recovery system based on the hybrid technique

By defining the conditions for each sub process in a closed process where the pickling acid is concentrated to over its saturation point for metals, and crystallised afterwards, it is possible to simulate the process regarding concentrations of metals in different baths as function of time. Thereby it is also possible to estimate steady state conditions.

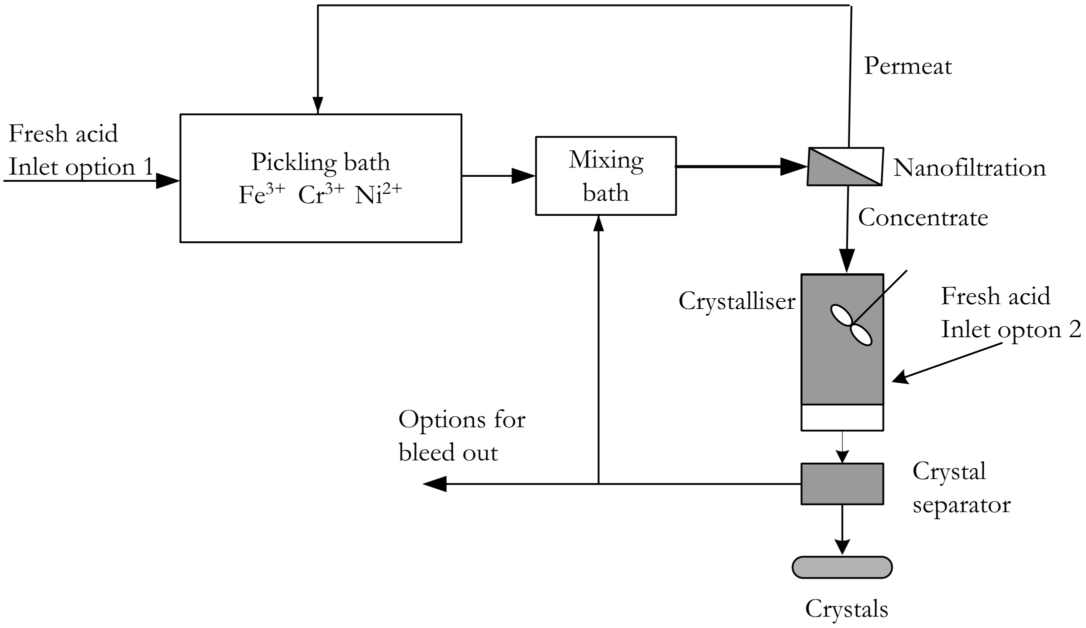

Figure 1. Illustration of a planned full-scale system for recovery of pickling acid.

The mass balance for the system can now be evaluated

Mass balance for the total process

For metals

Inlet + Production= Outlet + Accumulated

For the total system applies at steady state for metals, Inlet =0, and accumulation =0, this gives

Production = Outlet

For acids

For the total system applies at steady state for acids, Production = 0 and Accumulation = 0, this gives

Inlet = Outlet

Below the mass balances for iron is stated for each sub process.

Pickling bath

(1) $V_P * c_{perm} + prod = c_b *V_P$

c_b = content in pickling bath, g/l

prod = amount iron dissolved in the pickling bath g/h

V_P = permeatflow, l/h

(2) $c_{perm} = (1- R)* c_{conc}$,

$R=1- (c_{perm}/ c_{conc}) = 0.90$, for MPS34 and 0.40 for Nadir, at 40ºC anf 40 bar

(3) $V_P= f(c_{conc}, T, \Delta P) = 2358.1316055\ c_{conc}^{-1,9035700}$ (For the investigated MPS34 membrane, derived from experiments in this project)

(4) $V_T = V_P + V_K$

V_T = total into the nanofilter

The values used for the Nadir membrane are based on the experiment performed, which might be too positive values, if the same tendency as for the MP 34 membrane, i.e. to get less average flux, is valid.

Mixer bath

(5) $Inlet= P*c_b+V_K *c_{cryst}= V_T * c_{mix} = Out$

c_{mix} = Fe concentration out from the mixer, g/l

Nanofiltration

(6) $V_T * c_{mix} = V_P * c_{perm} + V_K * c_{conc}$

Crystallisation

(7) $V_K * c_{conc} = V_K * c_{cryst} + Cryst$

Cryst = amount crystallised , g/h

(8) *Prod = Cryst*

The following relation for crystallisation as function of iron concentration was used

Y = crystal growth per g seeds and second = $1.288287E^{-08}S^2 – 2.608852E^{-08}S + 1.327429E^{-08}$ (derived from experiments in this project)

Where S = super saturation. c/c*, where c* = saturation concentration

To be able to predict the crystallisation the magma density (kg metal fluorides per kg solution), the size of the crystals and the size of the crystallisation bath must be defined.

Mass balance of the total system

From the mass balances above for each sub process it is possible to calculate concentrations and flow in the whole system if certain parameters are decided. These are: production of iron (and other metals) by dissolution of stainless steel, total flow into the nano membrane, membrane area (and type of membrane), size of crystallisation unit, magma density and size of crystals. Also the amount acid blooded out from the system has to be defined.

Calculation procedure

The process is divided into sub processes, pickling bath, mixer, nanofiltration, and crystallisation unit. For each part of the system a concentration is estimated by assuming a plug flow under a certain time period (0.2-1 hours), followed by a total mixing of each bath at the end of each time period. This means that outflow from one tank is inlet to the next tank for the next time period. By following the concentration changes by time it is possible to estimate the concentrations at steady state, which will be reached after sufficient time. The calculations were performed with a developed spreadsheet.

To control that equilibrium really was reached it is possible to check the balances for in and out for each sub step.

The method will also give the possibility to follow dynamic changes by changes in inlet concentration and production.

Appendix 4. Pickling cases

SMT 8000 hours annual			**Annual**
	Dumped pickling acid	m^3	2156
Estimated	HNO_3	ton	323.4
Estimated	HF total	ton	109.6
Estimated	Metals total	ton	65.8
Estimated	Iron	ton	46.1
Estimated	Chromium	ton	11.8
Estimated	Nickel	ton	5.3
Estimated	CaO	ton	371
OKS 8000 hours annual			
Estimated	Dumped pickling acid	m^3	32000
	HNO_3	ton	1826
	HF	ton	726
	Metals total	ton	640
Estimated	Iron	ton	448
Estimated	Chromium	ton	115.2
Estimated	Nickel	ton	51.2
Estimated	CaO	ton	3600

Appendix 5. Results of simulation with the nanohybrid for the two sites

	Membrane/case	MP34 Case SMT	Nadir Case SMT	MP34 Case OKS	Nadir Case OKS
Inlet data	Amount pickling m^3 without recovery	2156	2156	32000	32000
	% reduction of acid	90%	86%	98%	98%
	Size of Pickling bath. m^3	3.84	3.84	37.33	37.33
	HF concentrate in pickling bath	1.75	1.75	3.00	3.00
	HNO_3 concentration in pickling bath	2.34	2.34	3.00	3.00
	Temperature in pickling bath	45.00	45.00	55.00	55.00
	Temperature in membrane and crystalliser	45.00	45.00	45.00	45.00
	Size of mixing bath	2.00	2.00	20.00	20.00
	Size of crystalliser. m^3	4.00	6.00	55.00	50.00
	Magma-density for crystalliser. weight %	15.00	15.00	15.00	15.00
	Membrane area in 1000 square meter	0.36	0.06	4.30	0.60
	Inlet flow into membrane m^3/h	1.80	5.00	18.00	45.00
	Out bleeding. m^3/h	0.026	0.038	0.072	0.072
	Out bleeding. m^3/annual	211.62	302.06	574.71	574.44
	Retention of metals	0.90	0.40	0.90	0.40
Calculated system conditions	Permeate-flow. m^3	0.35	1.87	4.14	16.12
	Iron-content in pickling bath. g/l	19.53	19.51	15.58	14.62
	Chromium-content in pickling bath. g/l	5.10	5.49	4.34	5.78
	Nickel-content in pickling bath. g/l	4.47	11.13	5.34	23.12
	Iron content in mixing bath. g/l	25.42	23.28	16.17	15.92
	Chromium content in mixing bath. g/l	7.18	6.66	6.83	6.98
	Nickel content in mixing bath. g/l	21.38	15.28	30.07	32.44
	Iron content in concentrate. g/l	30.82	27.38	20.38	18.58
	Chromium content in concentrate. g/l	8.70	7.83	8.61	8.15
	Nickel content in concentrate. g/l	25.93	17.97	37.90	37.87
	Iron content in crystalliser. g/l	26.85	25.54	16.34	16.65
	Chromium content in crystalliser. g/l	7.68	7.36	7.58	7.65
	Nickel content in crystalliser. g/l	25.47	17.76	37.44	37.65
	Supersaturation iron in crystalliser. c/c*	1.41	1.32	1.36	1.38
	Supersaturation chromium in crystalliser. c/c*	1.32	1.26	1.28	1.30
	Supersaturation nickel in crystalliser. c/c*	0.73	0.51	1.07	1.08
	Amount crystallised iron/hour	5.05	4.80	54.83	54.80
	Amount crystallised chromium/hour	1.28	1.21	13.86	13.86
	Amount crystallised nickel/hour	0.00	0.00	0.07	0.07
	Amount added acids m^3/hour	0.026	0.038	0.072	0.072
	ton HF added annual	77.85	83.72	687.09	691.43
	ton HNO_3 added annual	31.69	45.24	110.34	110.29
	ton Fe to neutralisation	5.68	7.71	9.39	9.56
	ton Cr to neutralisation	1.63	2.22	4.35	4.39
	ton Ni to neutralisation	5.39	5.36	21.52	21.63
	ton HF to neutralisation	14.26	18.83	50.77	53.68
	ton HNO_3 to neutralisation	31.69	45.24	110.34	110.29

Appendix 6. Energy data for chemicals

For lime the energy demand is estimated to be 8.95 GJ/ton, calculated on total primary energy use. Mining of lime and sea transports of carbon and lime included. Energy to produce the energy carrier and the energy losses in energy production and transmission are included as well. The energy for calcium burning stands alone for 6.3 GJ/ton (according to environmental report from Nordkalk).

For HNO_3 the primary energy use, including the energy for producing the energy carrier, is 13.6 GJ/ton. In this process the energy in natural gas, which is raw material for production of ammonia, is included.

For HF the amount is 33 GJ/ton. In this figure a long sea transport of fluorspar from China to Germany is included, as well as production of sulphuric acid and calcium oxide. For this process German average electricity mixture was applied.

The production of HF alone stands for 7.9 GJ/ton.

Reference: http://www.avestapolarit.com/upload/Avesta/ed/EnvironmentalEvaluation.pdf

Appendix 7. Estimation of investment costs for crystallisation

The estimated costs are given in SEK.

Size in m^3	**4**	**6**	**30**	**50**	**55**
GAP tank	50 000	60 000	270 000	500 000	500 000
Baffles and lock	15 000	18 000	81 000	150 000	150 000
Gear motor	100 000	100 000	400 000	550 000	550 000
In and outlet pump	20 000	20 000	50 000	50 000	50 000
Level sensors	10 000	10 000	10 000	10 000	10 000
Protection for acid leakage	8 000	8 000	20 000	20 000	20 000
Extra for montage	75 000	100 000	100 000	100 000	100 000
Sum	278 000	316 000	930 000	1 380 000	1 380 000

(GAP= glass fibre plastics)

Costs for connection of the crystallisation unit with the other equipment are not included in this table. The costs for GAP tank was obtained from JS Plastmontage, and cost for the gear motor was obtained from IKA process in Sweden. Other costs above were estimated.

Appendix 8. Mass balance.

The material balance for metals and acids for the 4 investigated cases:

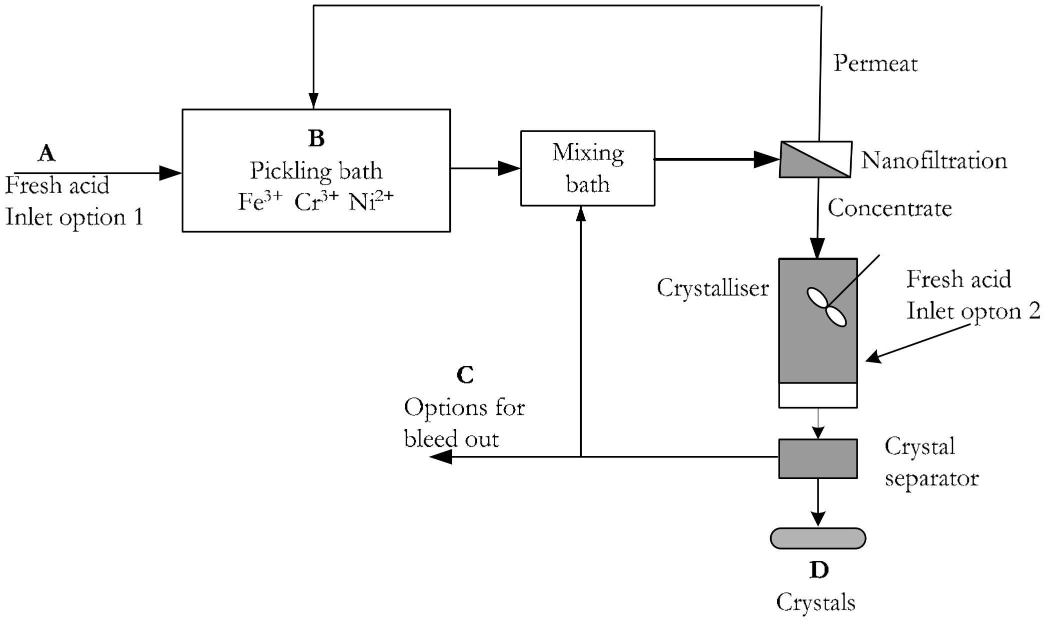

All values in kg/hour		Metals		
		B	C	D
		Produced	Crystals+liquid	Outblooded
MP34 Case SMT	Iron	5.76	5.29	0.46
	Chromium	1.48	1.35	0.13
	Nickel	0.67	0.23	0.44
Nadir Case SMT	Iron	5.77	4.94	0.83
	Chromium	1.48	1.24	0.24
	Nickel	0.67	0.09	0.58
MP34 Case OKS	Iron	56.00	55.80	0.20
	Chromium	14.41	14.31	0.09
	Nickel	2.76	2.30	0.46
Nadir Case OKS	Iron	56.00	55.79	0.20
	Chromium	14.41	14.31	0.09
	Nickel	0.20	2.32	0.46

		Acids		
		A	C	D
		Inlet	Crystals+liquid	Outblooded
MP34 Case SMT	HF	8.56	7.47	1.09
	HNO_3	3.96	1.37	2.59
Nadir Case SMT	HF	8.76	6.86	1.90
	HNO_3	5.65	0.78	4.87
MP34 Case OKS	HF	81.29	80.21	1.08
	HNO_3	13.79	11.44	2.35
Nadir Case OKS	HF	81.28	80.19	1.08
	HNO_3	13.79	11.44	2.35